THE JOURNAL OF COMPARATIVE NEUROLOGY 510:378–395 (2008)

Comprehensive Wnt-Related Gene Expression During Cochlear Duct Development in Chicken

ULRIKE J. SIENKNECHT AND DONNA M. FEKETE*
Department of Biological Sciences, Purdue University, West Lafayette, Indiana 47907

ABSTRACT

The avian cochlear duct houses both a vestibular and auditory sensory organ (the lagena macula and basilar papilla, respectively), which each have a distinct structure and function. Comparative mRNA in situ hybridization mapping conducted over the time course of chicken cochlear duct development reveals that Wnt-related gene expression is concomitant with various developmental processes such as regionalization, convergent extension of the cochlear duct, cell fate specification, synaptogenesis, and the establishment of planar cell polarity. Wnts mostly originate from nonsensory tissue domains, whereas the sensory primordia preferentially transcribe Frizzled receptors, suggesting that paracrine Wnt signaling predominates in the cochlear duct. Superimposed over this is the strong expression of two secreted Frizzled-related Wnt inhibitors that tend to show complementary expression patterns. *Frzb* (*SFRP3*) is confined to the nonsensory cochlear duct and the lagena macula, whereas *SFRP2* is maintained in the basilar papilla along with *Fzd10* and *Wnt7b*. Flanking the basilar papilla are *Wnt7a*, *Wnt9a*, *Wnt11*, and *SFRP2* on the neural side and *Wnt5a*, *Wnt5b*, and *Wnt7a* on the abneural side. The lateral nonsensory cochlear duct continuously expresses *Frzb* and temporarily expresses *Wnt6* and *SFRP1*. Characteristic for the entire lagena is the expression of *Frzb*; in the lagena macula are *Fzd1*, *Fzd7*, and *Wnt7b*, and in the nonsensory tissues are *Wnt4* and *Wnt5a*. Auditory hair cells preferentially express *Fzd2* and *Fzd9*, whereas the main receptors expressed in vestibular hair cells are *Fzd1* and *Fzd7*, in addition to *Fzd2* and *Fzd9*. J. Comp. Neurol. 510:378–395, 2008.

Indexing terms: Wnts; Frizzled; Wnt inhibitors; inner ear; basilar papilla; lagena

The inner ear of vertebrates contains several different sensory organs serving hearing and balance. In birds, one organ of each modality is located in close proximity in the cochlear duct. Thus two organs, the auditory basilar papilla (BP) and the vestibular lagena macula (LM), must become differentiated both anatomically and functionally during development. The BP is highly specialized for hearing and shows important spatial gradients (Gleich et al., 2004). Across the width of the organ (the radial dimension) is the axis of maximal sensitivity for hair cell bundle displacement, whereas along the length of the organ (the longitudinal dimension) is the tonotopic axis. Both axes show systematic changes in the mechanosensory hair cells and their innervation patterns (Fischer, 1994). Radially, columnal tall hair cells with relatively small luminal surfaces are situated on the neural (superior) side and give way to short hair cells with broad surfaces located on the abneural (inferior) side. Longitudinally, the lumenal transduction apparatus, the hair cell bundle, varies systematically from a tall, round shape with centrally placed stereocilia for low-frequency responses (in the distal apex) to short bundles with a wide rectangular shape for high frequencies (in the proximal base). Auditory hair cell bundles are coupled by a tectorial membrane.

The sensory epithelium of the lagena, situated in the distal end of the cochlear duct, rests on firm tissue. Its tall hair bundles are covered by a membrane containing otoconia similar to other vestibular maculae (Li et al., 2006). The avian LM consists mainly of uniform type II hair cells, except for two central stripes of loosely packed type I hair

Grant sponsor: National Institute of Deafness and Communication Disorders; Grant number: 002756 (to D.M.F.).

*Correspondence to: Donna M. Fekete, Department of Biological Sciences, Purdue University, West Lafayette, IN 47907.
E-mail: dfekete@purdue.edu

Received 18 January 2008; Revised 24 April 2008; Accepted 28 May 2008
DOI 10.1002/cne.21791
Published online in Wiley InterScience (www.interscience.wiley.com).

cells, which are restricted to the striola area (Rosenhall, 1970). Stereocilia bundles outside the striola region show an opposing polarity across the striola that reflects antiparallel directional sensitivity. Although there is still a profound lack of knowledge about the function of the LM, it has been shown that this cochlear vestibular organ has no auditory function (Manley et al., 1991a).

During ontogeny, the cochlear duct emerges from the ventral otocyst and is referred to as the pars inferior. The pars inferior includes prosensory domains that give rise to three sensory epithelia: the vestibular saccular and lagenar maculae, as well as the auditory BP. By midgestation, the pars inferior splits and the saccule segregates from the cochlear duct. Here we will focus on the cochlear duct, whereas a separate manuscript will present Wnt-related gene expression during the saccule's subsequent development together with the other sensory organs of the dorsal inner ear subdivision, the pars superior. By embryonic day 12 (E12, Hamburger and Hamilton stage 38, s38), cochlear differentiation has reached a state at which the hair cell types are distinguishable (Cohen and Fermin, 1978) and the inner ear becomes functional. Grier et al. (1967) demonstrated that embryonic chickens respond to sounds as early as E12, when compound action potential (CAP) thresholds are at high levels (Saunders et al., 1973; Rebillard and Rubel, 1981). Vanzulli and Garcia-Austt (1963) recorded microphonic potentials as early as E13.

Nonetheless, the hatchling BP is still immature both morphologically and functionally. Synaptogenesis as well as the achievement of final hair cell bundle orientation continues after hatching (Cohen and Fermin, 1978; Cotanche and Corwin, 1991). Between hatching and the first month, the cochlear duct lengthens by 16% (Ryals et al., 1984). Furthermore, intensity functions of primary auditory nerve fibers are not yet mature in post-hatched chickens (Manley et al., 1991b). Moreover, Jones and Jones (2000) found significant developmental changes occurring in the spontaneous activity of both lagenar and auditory neurons of the eighth cranial nerve between E19 and posthatch chickens.

Wnt-related gene expression in the inner ear has been reported previously (Hollyday et al., 1995; Jasoni et al., 1999; Stark et al., 2000; Daudet et al., 2002; Sajan et al., 2007), with functional data now emerging. Examples include the involvement of Wnts in early otic placode specification (Ohyama et al., 2006), Wnts mediating otic dorsalization from the adjacent hindbrain (Riccomagno et al., 2005; Hatch et al., 2007), cell autonomous β-catenin-mediated sensory fate specification (Stevens et al., 2003), and Wnt/Frizzled regulation of hair bundle planar polarity and cochlear duct elongation (Dabdoub et al., 2003; Wang et al., 2006; Qian et al., 2007). However, a comprehensive developmental sequence of Wnt-related gene expression in the cochlear duct, presented with topological mapping details, was previously lacking.

Wnt signaling pathways are highly conserved during evolution, and they seem to be repeatedly involved in various processes of development (and disease) across the animal kingdom. Wnt ligands elicit various responses via binding to a variety of Frizzled receptors and co-receptors, leading to the activation of distinct intracellular signaling pathways (see, e.g., Cadigan and Liu, 2006). Based on biochemical binding preferences and functional data, a classification of Wnt and Frizzled family members has been established. According to their ability to activate either a β-catenin-dependent canonical Wnt pathway or a planar cell polarity (PCP) or Wnt/Calcium pathway, they are classified into canonical and noncanonical signaling factors, respectively. However, recent evidence has shown that most Wnts bind to various Frizzleds and that the outcome of signaling is regulated by the receptor context rather than being intrinsic to a particular Wnt or Frizzled (Gordon and Nusse, 2006; Hendrickx and Leyns, 2008). For example, Wnt11, long viewed as a noncanonical Wnt, is clearly also able to signal via β-catenin in a Frizzled-LRP-dependent manner (Tao et al., 2005; Zhou et al., 2007). This functional plasticity has also been shown for Frizzleds. For example, *Fzd7* is required for *Xenopus* neural crest induction through canonical Wnt signaling, yet later neural crest migration is regulated by *Fzd7* together with *Wnt11* via a noncanonical pathway (Abu-Elmagd et al., 2006).

Furthermore, there can also be crosstalk between Wnt pathways. For example, during convergent extension, Wnt5a inhibits Wnt3a-induced canonical signaling (Schambony and Wedlich, 2007), yet in another context, Wnt5a can activate β-catenin via Fzd4 and LRP co-receptors (Mikels and Nusse, 2006). Additionally, repression of one pathway by another may occur through competition for a common receptor, as proposed by Maye et al. (2004), and via available ligand concentrations. Thus, Wnt expression could have an indirect effect in facilitating or blocking other Wnt signaling pathways, and Wnt antagonists, binding either to Wnts, Frizzleds, or co-receptors, become important to trigger the expression readout.

Therefore single expression patterns can be obscure, as they necessarily neglect the full expression context in which the proteins must function. This motivated us to undertake a comprehensive analysis of spatiotemporal gene expressions of Wnts, Frizzleds, and Wnt inhibitors during inner ear development. In this study we analyzed the expression of Wnt-related gene transcripts from outgrowth of the pars inferior (E4) through to an early functional auditory and vestibular organ (E15). The Results section describes many diverse expression patterns that coincide with key developmental events in the chicken cochlear duct.

MATERIALS AND METHODS

Tissue preparation

White Leghorn chicken eggs were incubated at 38°C in a humidified incubator up to the desired age. Embryonic stages were discriminated following Hamburger and Hamilton criteria (Hamburger and Hamilton, 1951). All embryonic tissue was handled in RNase-free conditions, fixed in 4% paraformaldehyde (PFA) in phosphate-buffered saline (PBS; pH 7.4; overnight at 4°C), and washed in PBS, pH 7.4. Immersion-fixed s24–s25 embryos were embedded intact to provide positive control tissues, such as limb buds, kidneys, eyes, etc., to confirm probe specificity. Embryos ranging from s26 to s37 were decapitated, and the heads were immersion fixed. From s37 onward, embryos were fixed via an intracardiac perfusion, and the heads were postfixed after removing the skin, dissecting the lower jaw, and tearing the tympanic membrane to facilitate fixation of the inner ear. These older stage ears were isolated by harvesting the cartilaginous temporal bone and removing ossified tissue by dissection before embedding and sectioning.

TABLE 1. Probe List With Numbers of In Situ Hybridization Tests per Developmental Stage Group[1]

		s24 | s26	s27 | s30	s31 | s36	s37 | s41
Wnt1	AY753286 1 – 373	2	5	6	1
Wnt2b	NM_204336 687 – 1067	1	4	4	1
Wnt3	NM_001081696 621 – 1034	5	8	20	15
Wnt3a	NM_204675 697 – 1088	3	6	12	8
Wnt4	NM_204783 798 – 1191	3	5	10	4
Wnt5a	NM_204887 994 – 1364	6	10	15	11
Wnt5b	NM_001037269 656 – 1017	4	4	10	5
Wnt6	NM_001007594 557 – 930	7	8	7	3
Wnt7a	NM_204292 555 – 1244 + 3'UTR	3	1	1	2
Wnt7b	NM_001037274 679 – 1067	2	4	13	8
Wnt8b	AY753292 440 – 834	2	4	7	3
Wnt9a	NM_204981 72 – 1132	4	9	14	11
Wnt11	NM_204784 1 – 1827	4	6	7	4

		s24 | s26	s27 | s30	s31 | s36	s37 | s41
Fzd1	NM_001030337 1148 – (1839)	3	4	7	5
Fzd2	NM_204222 288 – 1430	3	3	8	5
Fzd4	NM_204099 818 – 3757	3	8	7	5
Fzd7	NM_204221 1034 – 3090	3	6	10	6
Fzd8	XM_418566 728 – 1452	4	5	6	3
Fzd9	XM_425392 219 – 1746	5	3	16	13
Fzd10	NM_204098 1 – 2244	5	3	8	6
Dkk1	XM_421563 478 – 1064	4	2	6	4
Cer	NM_204823 44 – 877	4	5	6	2
SFRP1	NM_204553 250 – 468	4	6	11	5
SFRP2	NM_204773 1 – 1594	6	5	12	4
Frzb	NM_204772 655 – 1822	6	6	13	6

[1] Genes (accession number and sequence) for Wnt ligands, Frizzled receptors, and Wnt antagonists analyzed in this study on inner ear tissue from chicken embryos ranging from stage (s)24 to 41 (according to Hamburger and Hamilton, 1951) on embryonic day (E)4 to 15. Shaded in gray are genes that were not detected in ventral inner ear tissue *(Wnt1*, *Wnt2b*, and *Cer)*. Those three probes were not tested beyond s38 (E12).

Tissue was then cryoprotected (in 15% sucrose in PBS) and embedded in Tissue Freezing Medium (TFM; Triangle Biomedical Sciences, Durham, NC). Frozen serial sections of 15 μm were collected onto Superfrost Plus slides (Fisher Scientific, Fair Lawn, NJ). Depending on the developmental stage, consecutive sections were placed on a series of 10–20 slides. Every fifth section was probed with the same gene, which allowed for a comparison of five genes per specimen, including prosensory markers. Transverse and coronal sections were obtained by cutting angles parallel or perpendicular, respectively, to the longest dorsoventral axis of the otic anlage. Sections were stored at −80°C until use.

Preparation of probes

Riboprobes for chicken Wnts and Wnt-related genes (Chapman et al., 2004) were made from plasmids provided by the laboratories of G. Schoenwolf and C. Tabin. Sequencing and alignment confirmed the target genes (cf. Table 1). Table 1 provides information about 25 *Wnt* and Wnt-related genes that were studied, the number of experiments for each range of developmental stages, and whether expression was detected in the ventral ear. In addition, molecular markers such as *Ser1*, *Lfng* (Adam et al., 1998), *Msx1*, *BMP4* (Wu and Oh, 1996), and *FGF8* (Sanchez-Calderon et al., 2004) for developing chicken inner ear organs were probed on selected adjacent sections to identify prosensory domains. Antisense riboprobe for each gene was transcribed with either T3, T7, or SP6 RNA polymerase (Roche Applied Science, Indianapolis, IN) in the presence of digoxigenin-11-UTP (Roche Applied Science). Digoxigenin-labeled antisense RNA probes were purified with Centri-Sep spin columns (Princeton Separations, Adelphia, NJ) and precipitated with LiCl. Resulting probes were tested for RNA integrity by electrophoresis (1% agarose gel).

RNA in situ hybridization and visualization

In situ hybridizations were performed in parallel on sets of five slides with sequential sections to test different probes and marker genes on adjacent tissue sections, following a slightly modified protocol provided by M. Hidalgo-Sánchez (Sanchez-Calderon et al., 2005). Briefly, tissue sections were dried at 50°C, postfixed in 4% PFA, washed in PBS, digested for 10 minutes with Proteinase K (Roche Applied Science, 1 μg/ml), fixed in 4% PFA, washed

in PBS, and acetylated in 0.1 M triethanolamine with 0.25% Acetic anhydride, before permeabilizing with PBT (PBS with 0.1% Triton X-100). All steps, including the RNA hybridization, were performed with slides submerged in slide mailer boxes (Life Science Products, Frederick, CO). Sections were prehybridized in hybridization buffer without probe (2 hours at room temperature), before overnight hybridization at 72°C in formamide hybridization buffer (Sanchez-Calderon et al., 2005) containing riboprobe at ~1 μg/ml concentration.

Posthybridization washes were carried out in 2X SSC and 0.2X SSC first at hybridization temperature and then at room temperature. Anti-digoxigenin-AP Fab fragments (Roche Applied Science, 1:3,500) were used to detect hybridization, and alkaline phosphatase (AP) precipitation was performed with BM Purple AP Substrate (Roche Applied Science) for up to 3 days at varying incubation temperatures from 14° to 37°C. After stopping the precipitation (in 100 mM Tris, pH 7.5, 1 mM EDTA), the slides were either further processed immunhistochemically (see below) or dehydrated and coverslipped with ShurMount mounting medium (Triangle Biomedical Sciences).

Neurofilament immunhistochemistry

In addition to comparative in situ hybridizations with marker genes, double labeling with neurofilament-associated monoclonal 3A10 (Developmental Studies Hybridoma Bank [DSHB], University of Iowa, Ames, IA) was utilized to mark axons and aid the identification of prosensory epithelia (Adam et al., 1998; Sanchez-Calderon et al., 2004). 3A10 is a neurofilament-associated antigen raised in mouse against chicken ventral spinal cord and labels cells containing a phosphorylated neurofilament associated protein. Previously, Storey et al. (1992) used this antibody as a marker for embryonic chicken nervous tissue, and Perez et al. (1999) used it to reveal sensory neuron fate in the chicken embryo. Following a protocol modified after Sanchez-Calderon et al. (2004), supernatant from hybridoma cells containing anti-3A10 IgG_1 was diluted 1:50 with blocking solution. Blocking and antibody incubations were carried out in heat-inactivated 10% calf serum, 0.05% Triton X-100, 0.05% NaAzide in PBS. Biotinylated goat anti-mouse secondary antibody (IgG H+L; Vector, Burlingame, CA; BA-2000; 1:250) was used with extravidin-biotin-horseradish peroxidase complex (Vector ABC Standard Kit; 1:200). Peroxidase activity was revealed by using diaminobenzidine histochemistry. Negative controls confirmed that omission of the primary antibody prevented immunostaining.

Photomicrographic documentation

Photomicrographs of tissue sections were captured with a SPOT Flex color-mosaic camera (Diagnostic Instruments, Sterling Heights, MI) mounted on a Nikon E800 microscope. An image database (Apple software Aperture 2.1) was built to store and represent all in situ hybridization results (5,600 photomicrographs with key words). The figures in this study provide exemplary data to support the reported results. Cropping of photomicrographs and a minimal amount of contrast and brightness adjustment was done with Adobe (San Jose, CA) Photoshop CS3.

RESULTS

Ventral otic anlage, the pars inferior at stages 24 to 26 (E4–E5)

As the otic anlage begins to undergo morphogenesis, the ventral portion consists of the evaginating pars inferior. High mitotic activity characterizes its pseudostratified otic epithelium (Lang et al., 2000). Although not obviously segregated at this stage, the prosensory domains are arranged along the medial wall from proximal to distal in the following order: sacccular macula, BP, and LM. The first evidence of neurite ingrowth to the prosensory patches from the adjacent stato-acoustic ganglion begins on E4, with fibers penetrating the basal lamina (Knowlton, 1967). However, in the differentiating auditory receptor, the majority of fibers remain below the presumptive sensory epithelium until after E5 (Whitehead and Morest, 1985).

Prosensory. The prosensory medial wall of the pars inferior (Fig. 1A) as revealed by prosensory markers on consecutive serial sections and neurofilament labeling (compare Fig. 1B–D) is characterized by expressions of Frizzled genes. The details can be summarized as follows: *Fzd1* and *Fzd7* are most prominent in these domains (Fig. 1A, *Fzd7*, s25), followed by less intense *Fzd4* expression (not shown). By s26, *Fzd1* becomes weak in the BP primordium, whereas *Fzd4* and *Fzd7* continue to be relatively strong in the developing BP (Fig. 1E, *Fzd7*). Although also expressed medially, *Fzd2* is not as restricted to prosensory domains as the other receptor genes mentioned (not shown). *Fzd8* is expressed at relatively low levels in the pars inferior prosensory domains compared with its transcription in the vestibular prosensory patches of the dorsal ear (not shown). Exclusively expressed in the presumptive auditory receptor is *Fzd10* (Fig. 1G′), albeit not before s26. At that time, the elongation of the BP primordium is accompanied by complementary expression of particular inhibitor and receptor genes along and across the epithelium (Fig. 1E–H,J). In the neural-basal half of the BP primordium, where prospective hair cells and supporting cells leave the mitotic cycle first, *Fzd7* (Fig. 1E) and *Frzb* (Fig. 1F) are highly expressed, whereas they are transcribed weakly in the distal BP portion (Fig. 1G, bracket, shows this for *Frzb* in the same ear as in F). The latter area, where hair cells differentiate last, is where *Fzd10* (Fig. 1G′, bracket) is strongest, whereas *Fzd10* is absent in the neural-basal papilla (Fig. 1F′).

These locally concentrated expression patterns (summarized for *Frzb* and *Fzd10* in the schematic of the auditory epithelium, Fig. 1, center) roughly parallel the later developmental gradient of hair cell births on E5–E7 (Katayama and Corwin, 1989). Genes with asymmetric expression levels throughout the BP are marked with asterisks in the summary table in Figure 1. The stato-acoustic ganglion shows regional expression of *Fzd1*, *Fzd8*, and *Dkk1* by s26 (see Fig. 2I for *Fzd8*).

Of the *Wnt* genes, only *Wnt7a* and *Wnt9a* are expressed transiently within prosensory patches of the pars inferior at s25 (Fig. 1I shows this for *Wnt7a*), although this expression is weak compared with positive control tissue elsewhere in the embryo (not shown).

Nonsensory. The nonsensory pars inferior expresses mostly *Wnt*s, whereas *Frizzled*s are expressed in the prosensory domains (see above). Based on the pattern of gene expression domains that are evident in our samples,

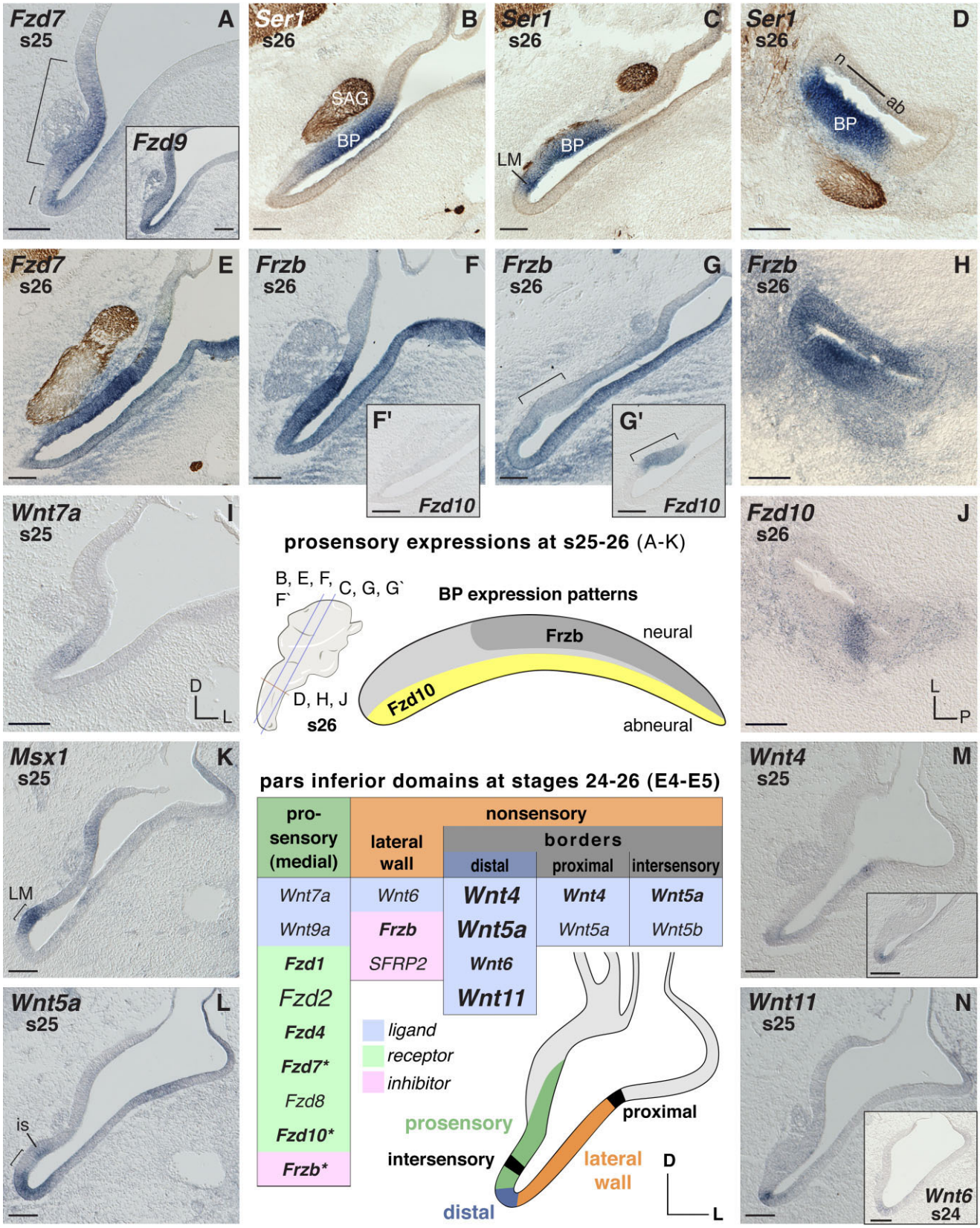
Fzd7 s25 A
Fzd9
Ser1 s26 B
SAG
BP
Ser1 s26 C
BP
LM
Ser1 s26 D
n
ab
BP
Fzd7 s26 E
Frzb s26 F
F'
Fzd10
Frzb s26 G
G'
Fzd10
Frzb s26 H
Wnt7a s25 I
D
L
prosensory expressions at s25-26 (A-K)
B, E, F, F`
C, G, G`
D, H, J
s26
BP expression patterns
Frzb
neural
Fzd10
abneural
Fzd10 s26 J
L
P
Msx1 s25 K
LM
pars inferior domains at stages 24-26 (E4-E5)
pro-sensory (medial)
nonsensory
lateral wall
borders
distal
proximal
intersensory
Wnt7a
Wnt9a
Fzd1
Fzd2
Fzd4
Fzd7*
Fzd8
Fzd10*
Frzb*
Wnt6
Frzb
SFRP2
Wnt4
Wnt5a
Wnt6
Wnt11
Wnt4
Wnt5a
Wnt5a
Wnt5b
ligand
receptor
inhibitor
prosensory
intersensory
distal
proximal
lateral wall
D
L
Wnt4 s25 M
Wnt5a s25 L
is
Wnt11 s25 N
Wnt6 s24

Figure 1

we have divided the nonsensory regions into the lateral wall of the ventral otic epithelium and several border domains (described separately below).

Wnt6 is initially concentrated at the distal tip of the pars inferior (at s24; Fig. 1N, inset) before increasing in abundance along the full length of the lateral wall by s25 (for later stage, see Fig. 2F). *Frzb* and *SFRP2* overlap in the nonsensory lateral wall at s24–s25 (not shown). However, by s26 *Frzb* represents the dominant *Wnt*-inhibitor gene found along the lateral pars inferior (Fig. 1G).

Borders. The most prominent Wnt expression domain in the ventral otic anlage at s24–s26 is the distal tip of the pars inferior, which forms a border between the prosensory patch of the LM, revealed by the marker probe *Msx1* (cf. Wu and Oh, 1996) (Fig. 1K), and the nonsensory lateral wall. *Wnt5a* (Fig. 1L), *Wnt4* (Fig. 1M, inset), *Wnt11* (Fig. 1N), and *Wnt6* (Fig. 1N, inset) are each expressed in this distal domain. Another border is established proximally by *Wnt4* (Fig. 1M) and *Wnt5a*, flanking the prosensory patch of the utricular macula at the junction of pars inferior and superior. Finally, on the medial side, *Wnt5a* (Fig. 1L) and *Wnt5b* flank the lagenar sensory patch; we have designated this region as the "intersensory" border (Fig. 1L, is).

Broad epithelial expression patterns. Several genes are expressed broadly throughout the pars inferior while also showing a more intense signal near the apical (lumenal) surfaces of the otic epithelium at s24–s25. These include *Dkk1*, *Fzd9* (Fig. 1A, inset), *Wnt7b*, and *Wnt9a*. Due to the absence of regionally restricted expression, these genes are not all listed in the summary table of Figure 1.

Periotic mesenchyme. With the exception of *Fzd1* (not shown), there is no specific Wnt-related gene expression in the mesenchyme adjacent to the pars inferior at s24 and s25. However, from s26 onward, several genes are found. *Fzd1*, *Fzd8*, and the *Wnt*-inhibitor gene, *Frzb*, are strongly expressed in the periotic mesenchyme, with the latter being especially prominent lateral and ventral to the pars inferior (Fig. 1F,G). Moderate levels of *Fzd7*, *Fzd9*, and *Dkk1* transcripts are present in the periotic mesenchyme (Fig. 1E shows *Fzd7*). In addition, the mesenchyme of the presumptive middle ear anlage has a high accumulation of *SFRP2* transcripts (Fig. 2A).

Pars inferior at stages 27–32 (E5–E7)

By E5 (s27), the developing inner ear has undergone substantial dorsoventral expansion. The lumen of the cochlear duct maintains a broad communication with the lumen of the saccule until the junction begins to constrict at E7.5 (s32; Cohen and Cotanche, 1992). The BP and the LM do not separate until E6.5 (s30) based on *BMP4* as a molecular marker for sensory primordia (Wu and Oh, 1996). However, the distal expression of both *Msx1* (s25) and *FGF8* (s27) suggest that LM specification takes place earlier, even if segregration of the organs is not yet completed (see Fig. 1K and Sanchez-Calderon et al. 2004). Anatomically, the auditory receptor primordium can first be identified at late E5–E6 (s28–s29) (Cohen and Cotanche, 1992). E5–E6 is when the first hair cell and supporting cell progenitors of the presumptive auditory organ leave the mitotic cycle (Katayama and Corwin, 1989). Cell differentiation, as detected by hair cell antigen (HCA), begins at E5 (s27) in the vestibular saccular macula, and at E6 (s29) in the LM/BP (Bartolami et al., 1991) with just a few cells visible. According to Whitehead and Morest (1985) during E5–E7 (s27–s31), there is a phase of massive neurite ingrowth, when most of the ganglion cell fibers invade the sensory primordia.

Prosensory. *SFRP2* displays the most striking Wnt-related gene expression in the BP, with the highest concentration in the middle and distal regions of this developing epithelium (Fig. 2A). All tested *Frizzled* receptors are transcribed in the prosensory pars inferior in a differential manner, whereas none of the *Wnt* ligand genes are particularly evident there between s27 and s32. The three presumptive sensory organs have partly overlapping *Frizzled* expression patterns.

The auditory primordium shows expression of *Fzd4*, *Fzd7*, and the aforementioned unique and regional *Fzd10*

Fig. 1. Ventral ear (pars inferior) mRNA expression between s24 and s26 (E4–E5). In situ hybridization signals (purple) are exemplarily counterstained by labeling of neurofilament (brown) with neurofilament-associated 3A10 antibody in sample images. **A–K:** Expression in prosensory pars inferior areas. Brackets in A demarcate prosensory regions of the medial pars inferior. **A, inset:** Broad expression of *Fzd9* in the ventral otic anlage. **B–D:** Two independent markers reveal prosensory areas: *Ser1* (purple), and for neuronal processes, NF-antibody 3A10 (brown). **B,C:** Two section levels of the same ear through the anterior-basal half and posterior-distal basilar papilla (BP) plus lagenar macula (LM), respectively. **E,F,F′:** Anterior section level through the neural-basal half of the BP showing strong expression of *Fzd7* and *Frzb*, whereas *Fzd10* (F′) is negative in the neural-basal half of the BP. **G,G′:** Posterior section level through the abneural pars inferior and the distal BP (bracket) of the same ear, respectively, showing weak *Frzb* and distinct *Fzd10* expression. **F,G:** Lateral nonsensory pars inferior expresses *Frzb*. **H,J:** Cross sections reveal local concentration of *Frzb* and *Fzd10* transcripts in the BP (compare with D; these three are consecutive sections of the same ear). **H:** Lateral nonsensory pars inferior expresses *Frzb*. BP shows *Frzb* expression gradient with highest concentration in the anterior-neural two-thirds. **J:** Local expression of *Fzd10* in the abneural BP. **I:** Weak expression of *Wnt7a* in the prosensory pars inferior. **K:** *Msx1* probe used as a marker to reveal the LM prosensory patch (bracket). **L–N:** *Wnt* expression in border domains. **L:** *Wnt5a* transcripts flank the LM (bracket) (compare with K). Abbreviations: ab, abneural; BP, basilar papilla; D, dorsal; is, intersensory domain; L, lateral; LM, lagenar macula; n, neural; P, posterior; s, stage; SAG, stato-acoustic ganglion. Center: Orientation and section levels for s26 images are indicated in the cartoon of the otic anlage, lateral view (left); a map of the complementary gene expressions (*Frzb* and *Fzd10*) is shown in the schematic outline of the BP (right). **Summary table s24–s26 (E4–E5):** Otic epithelium domains express the listed genes. Table headers refer to otic domains shown in the color-coded schematic. Gene expression over the summarized time span is categorized by different font sizes and font faces to indicate distinct versus weak or temporally varying expression, as follows. Font face (bold/plain) refers to signal strength: bold indicates obvious (high signal-to-noise) labeling; plain indicates weaker detection or lower signal-to-noise labeling. Relative signal strengths may be probe dependent and do not necessarily reflect quantitative differences across probes. Font size (small/large) refers to either duration of the expression or local restriction: small means not continuously expressed over the time window covered in this panel description *or* the gene is expressed only in particular regions of that domain; large refers to broad expression within the domain. Summary table s24–s26 (E4–E5) does not list *Dkk1*, *Fzd9*, and *Wnt7b*, which are broadly expressed in the ventral otic anlage and therefore are not specific for a particular domain. Asterisks label genes with local expression or a gradient along and across the BP primordium (see text). Scale bar = 100 μm.

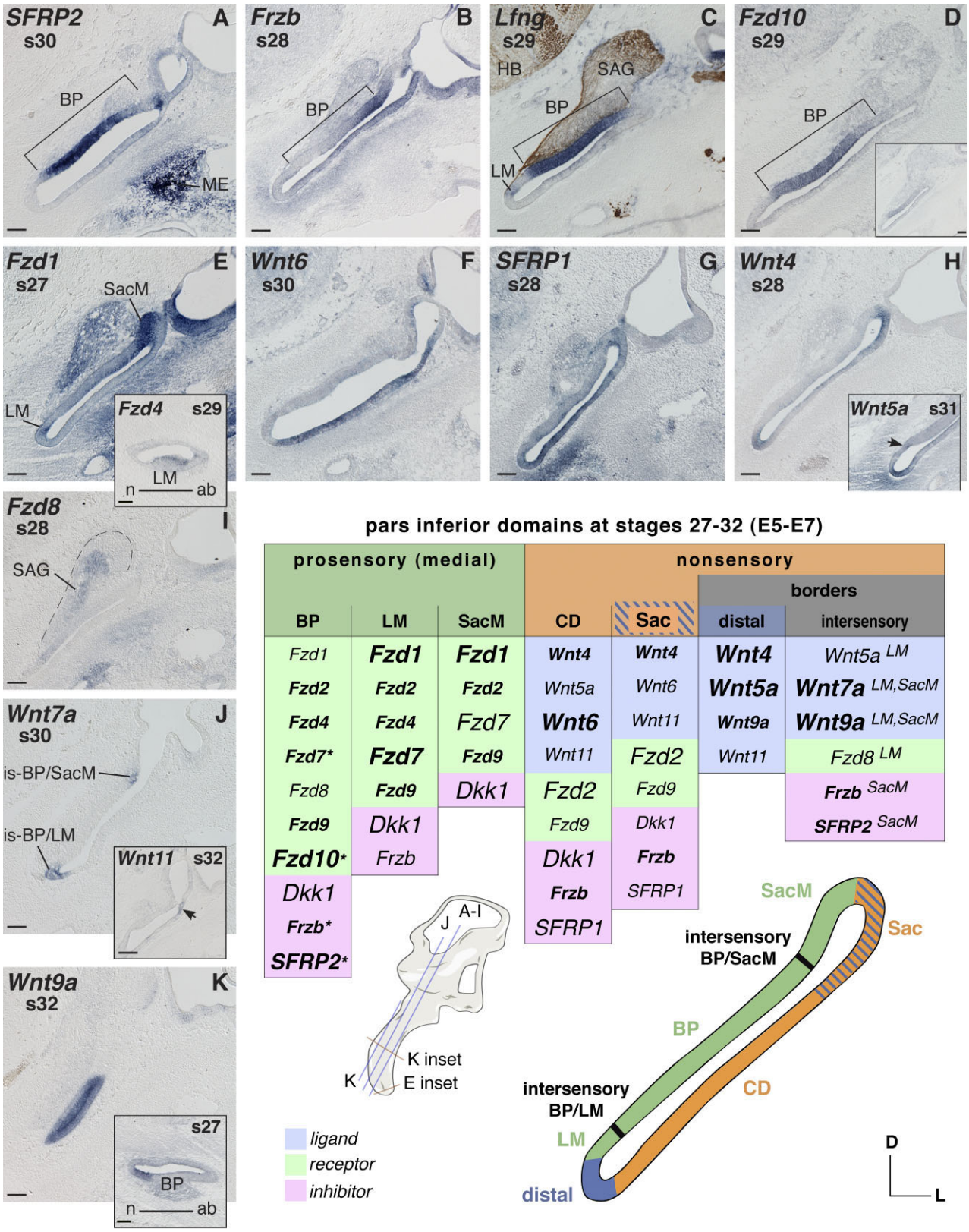
SFRP2 s30 A
BP
ME
Frzb s28 B
BP
Lfng s29 C
HB
SAG
BP
LM
Fzd10 s29 D
BP
Fzd1 s27 E
SacM
LM
Fzd4 s29
LM
n
ab
Wnt6 s30 F
SFRP1 s28 G
Wnt4 s28 H
Wnt5a s31
Fzd8 s28 I
SAG
Wnt7a s30 J
is-BP/SacM
is-BP/LM
Wnt11 s32
Wnt9a s32 K
s27
BP
n
ab
pars inferior domains at stages 27-32 (E5-E7)
prosensory (medial)
nonsensory
borders
BP
LM
SacM
CD
Sac
distal
intersensory
Fzd1
Fzd2
Fzd4
Fzd7*
Fzd8
Fzd9
Fzd10*
Dkk1
Frzb*
SFRP2*
Fzd1
Fzd2
Fzd4
Fzd7
Fzd9
Dkk1
Frzb
Fzd1
Fzd2
Fzd7
Fzd9
Dkk1
Wnt4
Wnt5a
Wnt6
Wnt11
Fzd2
Fzd9
Dkk1
Frzb
SFRP1
Wnt4
Wnt6
Wnt11
Fzd2
Fzd9
Dkk1
Frzb
SFRP1
Wnt4
Wnt5a
Wnt9a
Wnt11
Wnt5a LM
Wnt7a LM,SacM
Wnt9a LM,SacM
Fzd8 LM
Frzb SacM
SFRP2 SacM
J
A-I
K
K inset
E inset
ligand
receptor
inhibitor
SacM
Sac
intersensory
BP/SacM
BP
CD
intersensory
BP/LM
LM
distal
D
L

Figure 2

(Fig. 2D,D inset). Less distinctly expressed is *Fzd2*, and the BP transcribes weakly *Fzd1* and *Fzd8* (Fig. 2E,I). From s32, *Fzd9* is expressed in the domain of differentiating sensory progenitor cells in the superficial layer of the BP (Fig. 3D, s34). The localized expression along and across the developing BP described earlier is maintained until at least s29 (E6). That is, *Fzd7* and *Frzb* are highest in the neural-base (Fig. 2B, *Frzb*) in a complementary fashion to *SFRP2* (Fig. 2A) and *Fzd10* (Fig. 2D). Comparison with prosensory marker gene expression (*Lfng*) (Fig. 2C) reveals further a gradual change from weak *Fzd10* transcription in the middle BP to a robust expression in the middle-to-abneural BP (see Fig. 2C, *Lfng*, and the adjacent section level of the same embryo probed for *Fzd10*, Fig. 2D, inset, compared with *Fzd10* in the slightly more posterior middle-to-abneural BP, Fig. 2D). At s30, the gradients of *Fzd7* and *Frzb* are lost and both become confined to only the BP base (not shown). In contrast, the domains of *Fzd10* and *SFRP2* (Fig. 2A) are maintained. *Fzd10* continues to be excluded from the neural BP, where the expression of *SFRP2* is also weak (Fig. 2A).

The lagenar primordium can be distiguished by a local increase in the transcription of the prosensory marker *Lfng* (LM in Fig. 2C) as well as *Fzd1* (Fig. 2E) and *Fzd7* (not shown). Although initially broad within the LM, *Fzd4* becomes confined to the presumptive hair cell layer at s29 (E6; Fig. 2E, inset). This cellular specificity at s29 and thereafter is also apparent for *Fzd2*, *Fzd9*, and the other lagenar-expressed *Fzd* genes (see, e.g., Fig. 3D,G). In addition to the receptors, *Frzb* shows lagenar transcripts, but rather weakly until after s30 (E6.5; described later, Fig. 3I).

For the prosensory saccule, a robust expression of *Fzd1* (Fig. 2E) is accompanied by locally concentrated *Fzd2* and some *Fzd7*, fading in from the adjacent BP domain (not shown).

The stato-acoustic ganglion expression of *Fzd1*, *Fzd8*, and *Dkk1* mentioned earlier continues into s27–s29 (Fig. 2I shows this for *Fzd8* and Fig. 2E for *Fzd1*).

Broad expression in the pars inferior is displayed by *Fzd2*, *Fzd9*, and also *Dkk1*, although they seem to concentrate locally in the forming hair cell layer (for *Dkk1* this localization becomes more obvious by s33/34; data not shown). For example, the weak and broad expression of *Fzd9* begins to be confined to the apical layer in all three prosensory epithelia at s32 and later (see further in the description of the next stages).

Nonsensory. *Wnt6* and *SFRP1* are present along the lateral pars inferior (Fig. 2F,G). An inverse expression pattern is apparent for *Wnt4* (Fig. 2H) compared with *Wnt6*. As a result, although *Wnt4* and *Wnt6* are broadly overlapping, *Wnt6* expression characterizes the nonsensory cochlear duct, whereas *Wnt4* expression is more characteristic of the forming nonsensory saccule (proximal) and the nonsensory lagena (distal). Particularly at s29 (E6), *Wnt5a* appears to temporarily extend its otherwise more constricted distal occurrence to an expression along the entire nonsensory pars inferior (not shown). Then, from s31 (E7) onward, the cochlear *Wnt5a* expression is again confined to the nonsensory lagena (Fig. 2H, inset). *Frzb* becomes the predominant expressor antagonist in the entire nonsensory pars inferior from s30 (E6.5) onward (Fig. 3I). Faintly and sporadically, *Wnt11* transcripts are detectable in the nonsensory saccule and, particularly at s32, also in the adjacent proximal cochlear duct (Fig. 2J, inset). In addition, there is a singular occurrence of weak *Wnt7b* expression in the nonsensory saccule at s30 (E6.5; data not shown): the transcript is not detectable in this tissue at earlier or later time points. Instead, it is upregulated in sensory epithelia from s34 (E8) onward (see description of next developmental stages).

Borders. Based on Wnt-related gene expression compared with molecular markers for prosensory domains, several border domains are apparent in the pars inferior at s27–s32. These are: 1) a distal domain that differentiates into the nonsensory lagena; 2) a proximal region where the forming nonsensory saccule is connected to the nonsensory cochlear duct (see under "Sac" in Fig. 2 summary table); two "intersensory" domains bordering the differentiating BP, on one side 3) toward the primordium of the LM (intersensory BP/LM), and on the other side 4) toward the macula of the saccule (intersensory BP/SacM); and finally 5) the anterior flank of the pars inferior bordering the neural BP (not represented in the summary table). Expression in these border domains is as follows:

1. The distal pars inferior expresses *Wnt4* (Fig. 2H), *Wnt5a* (Fig. 2H, inset), and faintly *Wnt11* (not shown). From s32 (E7.5) onward, *Wnt9a* is transcribed in this domain, although the expression is relatively weak compared with its occurrence in the intersensory domains (see below).
2. The nonsensory tissue connection between the saccule and the cochlear duct expresses *Wnt11* at s32 (E7.5), a

Fig. 2. Pars inferior mRNA expression between s27 and s32 (E5–E7). **A–E:** Prosensory expression. **A,B,D:** Basilar papilla (BP) expresses *SFRP2* and regionally *Frzb* and *Fzd10*. **C:** Double labeling by using *Lfng* probe as prosensory marker and neurofilament-associated antibody 3A10 reveals innervated prosensory areas. **C,D,D inset:** Adjacent tissue sections of the same embryo probed for *Lfng* or *Fzd10*. **D:** Robust expression of *Fzd10* in the distal and abneural-middle part of the BP. **D, inset:** *Fzd10* weakly expressed in the middle-to-neural BP on an adjacent slightly more anterior section level. **E,E inset:** Frizzled expression in vestibular prosensory domains. **E:** Maculae of the saccule and the lagena transcribe *Fzd1*. **E, inset:** Cross section through the distal cochlear duct (CD) shows *Fzd4* expression in the lagenar macula (LM). **F–H:** *Wnt* and *SFRP1* gene transcripts in the nonsensory pars inferior (nonsensory CD and Sac). **H, inset:** *Wnt5a* expression 1) in the periotic mesenchyme at the distal tip of the CD; 2) the intersensory region between BP and LM (arrow); and 3) the distal nonsensory LM. **I:** *Fzd8* regionally expressed in the SAG (outlined by dashed line). **J,K:** Border domains expressing *Wnt7a* and *Wnt9a*. **J, inset:** *Wnt11* positive region (arrow) at the junction of nonsensory Sac and CD. **K:** Anterior (neural) pars inferior expresses *Wnt9a*; **K, inset:** Cross section through the cochlear duct, showing this neural CD localization of *Wnt9a* transcripts at a younger stage of development. Abbreviations: ab, abneural; BP, basilar papilla; CD, cochlear duct; D, dorsal; HB, hindbrain; is, intersensory; L, lateral; LM, lagenar macula; ME, middle ear; n, neural; s, stage; Sac, saccule; SacM, saccular macula; SAG, stato-acoustic ganglion. Orientation and section levels are indicated in the 3D cartoon of the otic anlage, lateral view. **Summary table s27–s32 (E5–E7):** See legend to Figure 1 for explanation and font conventions. Asterisks label genes with local expression or a gradient along and across the BP primordium (see text). Scale bar = 100 μm.

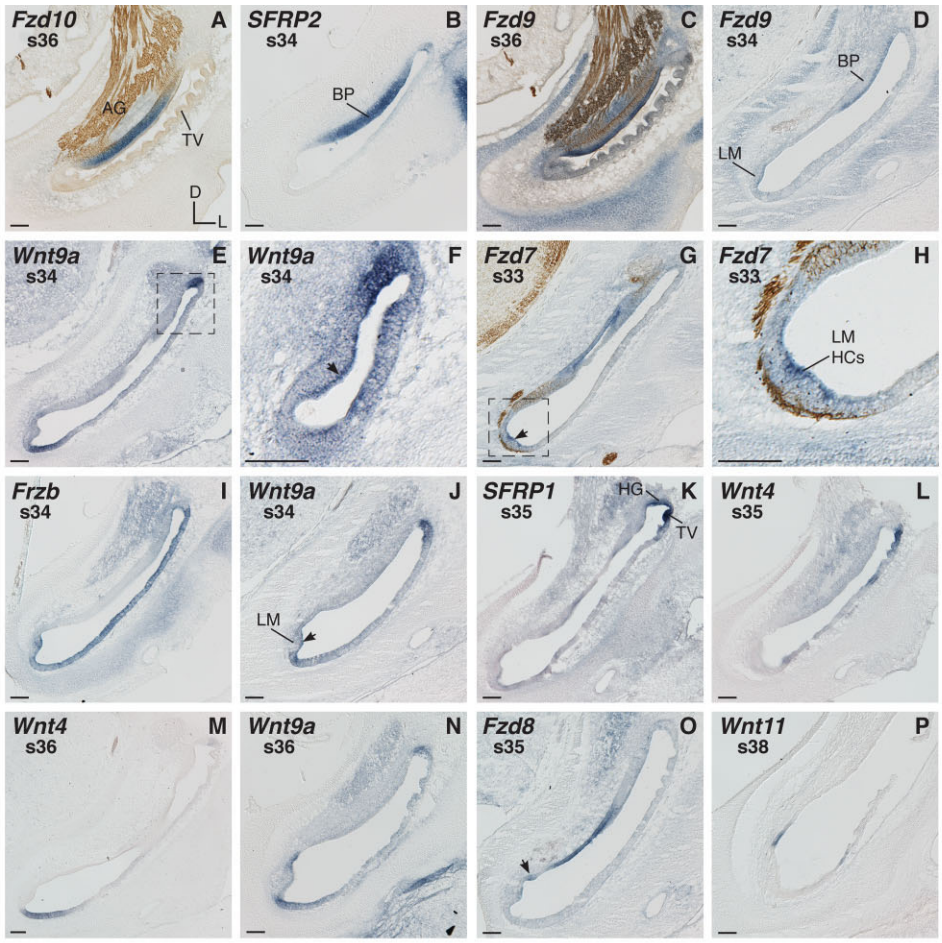

cochlear duct domains at stages 33-36 (E8-E10)

sensory CD		nonsensory CD				
		lateral	distal	proximal	borders	
BP	LM	wall	n-s Lag	TV origin	CD / Sac, HG	intersensory
Wnt7b	***Wnt7b***	***Wnt6***	***Wnt4***	***Wnt4***	*Wnt4*	*Wnt4*
Wnt9a	*Wnt8b*	***Wnt9a***	***Wnt5a***	*Wnt6*	***Wnt7a***	***Wnt7a***
Fzd1	*Wnt9a*	***Fzd2***	*Wnt6*	*Wnt7b*	***Wnt9a***	***Wnt9a***
Fzd2	***Fzd1***	***Fzd9***	***Wnt9a***	***Wnt11***	***Wnt11***	*Wnt11*
Fzd4	***Fzd2***	***Dkk1***	***Wnt11***	*Fzd2*	***SFRP1***	***Fzd8***
Fzd7	*Fzd4*	***Frzb***	*Fzd4*	*Dkk1*	***SFRP2***	
Fzd8	***Fzd7***	*SFRP1*	*Frzb*	***Frzb***		
Fzd9	*Fzd8*			***SFRP1***		
Fzd10	***Fzd9***					
Dkk1	***Dkk1***					
Frzb	***Frzb***					
SFRP2	*SFRP1*					

ligand
receptor
inhibitor

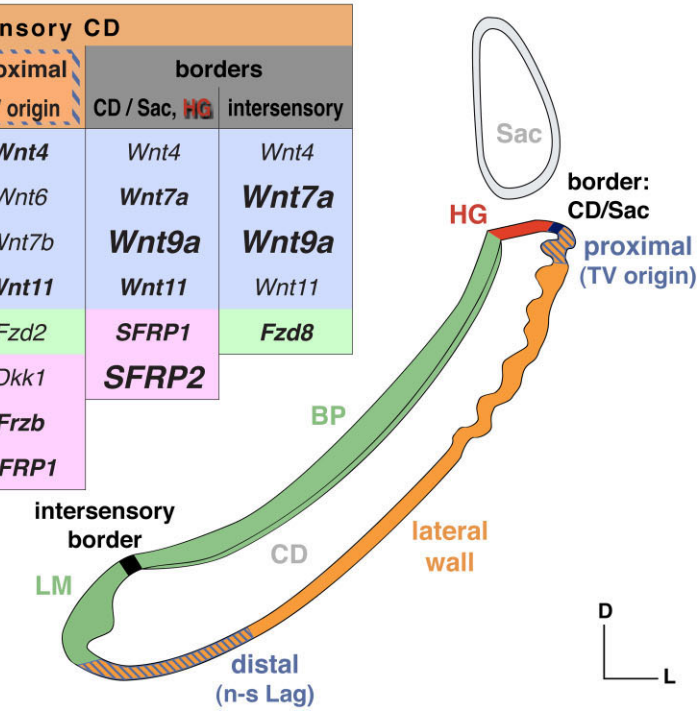

Figure 3

time when the communication between both organ compartments begins to constrict (Fig. 2J, inset).

3. The intersensory BP/LM strongly expresses *Wnt7a* (Fig. 2J) and *Wnt9a* (not shown). A faint demarcation is visible also by detection of *Wnt5a* transcripts in this tissue at s31 (see arrow in Fig. 2H, inset). In addition to prosensory markers, differential receptor gene expression patterns demarcate the intersensory BP/LM domain as follows: the expression of *Fzd4* (s28) and *Fzd7* leaves a gap along the medial wall (see Fig. 1A for *Fzd7* at an earlier stage). *Fzd8* fills this gap with its "intersensory" expression at s28 (data not shown; see a similar pattern later, in Fig. 3O), although this receptor gene is rather weakly transcribed in the entire ventral ear in the period of s27–s32 (Fig. 2I).
4. The intersensory BP/SacM domain, proximal to the auditory organ, resembles the BP/LM domain in that *Wnt7a* and *Wnt9a* are both expressed in this region (Fig. 2J shows this for *Wnt7a*). In addition, this junction transcribes *Frzb* (Fig. 2B) and *SFRP2* (Fig. 2A).
5. The two intersensory borders are interconnected via an expression domain flanking the auditory epithelium along its entire anterior-neural side, evidenced by a continuous expression of *Wnt7a* and *Wnt9a* (Fig. 2K). This domain abuts the cochlear nonsensory expression of *Wnt4* and *Wnt6* (described above). Cross sections through the cochlear duct probed for *Wnt9a* reveal this asymmetric neural expression domain adjacent to one side of the developing BP (Fig. 2K, inset).

Broad epithelial expression patterns. Between s27 and s32 (E5–E7), several genes are broadly expressed in the ventral ear; these are *Dkk1*, *Fzd2*, and *Fzd9*.

Periotic mesenchyme. The mesenchyme surrounding the cochlear duct shows transcripts in various intensity of all *Frizzled*s (Fig. 2E,I and see, e.g., Fig. 3C), with the exceptions of *Fzd4* and *Fzd10* (cf. Fig. 3A for *Fzd10*). Also present are transcripts for three Wnt-antagonists, *Frzb* (Fig. 2B), *SFRP1* (Fig. 2G), *Dkk1*, and one ligand, *Wnt5a* (Fig. 2H, inset). *Frzb* localizes in condensing mesenchyme around the distal and lateral cochlear duct (Fig. 2B). Other local concentrations are apparent: *Wnt5a* is strongly expressed in the mesenchyme surrounding the distal tip of the cochlear duct (Fig. 2H, inset); transcripts of *SFRP1* are found in the periotic mesenchyme of the ventral-lateral half of the pars inferior (Fig. 2G), whereas *Fzd1* shows expression only laterally but not distally (Fig. 2E). All transcripts leave a negative hollow immediately adjacent to the otic epithelium (Fig. 2B,G shows that for the inhibitor genes). This becomes particularly striking around s32 (E7–E8), when cartilage condensation takes place. More distant from the cochlear duct, the fourth Wnt-antagonist gene, *SFRP2*, is remarkably strong in the condensing mesenchyme of the forming middle ear (Fig. 2A), as described for younger stages.

Cochlear duct at stages 33–36 (E8–E10)

The ventral ear, described so far as the pars inferior, separates into the saccule and the cochlear duct. By E8/9 (s35), the communication between the two compartments constricts and narrows, so that both are finally interconnected solely by the ductus reuniens (Cohen and Cotanche, 1992).

Tissue specification leads to formation of the tegmentum vasculosum, a tissue that is thought to be responsible for the endolymph ionic composition and the endocochlear potential. The first tegmentum-folds form in the proximal cochlear duct at E8/E9 (s35) and then subsequently progress throughout its entire length to the nonsensory lagena (Cotanche and Sulik, 1982). Tissue that consists of homogene and clear cells becomes functional at E9 (~s35) and contributes to the forming tectorial membrane by secretion of the second layer matrix, according to Shiel and Cotanche (1990). Finally, the completion of the tectorial membrane coincides with the opening of the perilymphatic spaces (Fermin and Cohen, 1984), which according to our data is evident at s36-37 (E10-E11).

Between E8 and E10 (s34–s36), auditory hair cells begin to mature systematically both across and along the BP. Whereas hair cell production initiates in the middle and neural side (Katayama and Corwin, 1989), biased stereociliary bundle orientation to achieve planar cell polarity starts along the abneural (inferior) BP between E9 and E11 (Shiel and Cotanche, 1990). Spatially and temporally this coincides with the differentiation of short hair cells in the abneural BP (see below description of cell differentiation).

Sensory. The BP and LM display distinct mRNA expression patterns. A core set of genes, *Fzd10* (Fig. 3A), *SFRP2* (Fig. 3B), *Wnt7b*, and *Fzd9* (Fig. 3C,D), characterizes the differentiating BP. This "core set" is joined in a broader and less specific manner by all other receptor genes studied, as well as *Dkk1*. At s34, transcript localization of *Wnt9a* occurs in the BP, where hair cells differentiate (Fig. 3E,F). *Frzb* refines its expression to the nonsensory cochlear duct (and the LM) by s35, finally excluding the auditory epithelium. However, at s34, although most of the BP is already negative for *Frzb*, the neural mid-base still expresses this Wnt-antagonist gene (Fig. 3I). Thus, the region of strongest *Frzb* expression earlier remains positive the longest.

Locally concentrated mRNA expression is striking across the width of the differentiating auditory epithelium (summarized in the summary table in Fig. 4). *SFRP2* shows a central expression, peaking in the middle of the

Fig. 3. Cochlear duct mRNA expression between s33 and s36 (E8–E10). **A–D:** *Frizzled* and *SFRP2* expression in the basilar papilla (BP). **A,B:** BP supporting cell domain transcribes *Fzd1* and *SFRP2*. **C,D:** Hair cells express *Fzd9*. **E:** *Wnt9a* expression 1) in the presumptive homogene cell domain in the proximal CD (frame); and 2) in the nonsensory lagena at the distal end of the CD. **F:** Hair cells (arrow) in the basal BP transcribe *Wnt9a* at s34 (see frame in E, adjacent section). **G–J:** LM hair cells transcribe *Fzd7*, *Frzb*, and *Wnt9a*. **H:** Detail magnification of LM (frame in G). **I:** *Frzb* labels the entire nonsensory cochlear duct and the LM. **K,L:** Transcripts of *SFRP1* and *Wnt4* in the proximal CD. **M–P:** Transcripts bordering the LM. **O:** *Fzd8* expressed in the abneural border flanking the long axis of the BP. The arrow marks the intersensory border. Abbreviations: AG, auditory ganglion; BP, basilar papilla; CD, cochlear duct; D, dorsal; HCs, hair cells; HG, homogene cell domain; L, lateral; LM, lagenar macula; n-s Lag, nonsensory lagena; Sac, saccule; s, stage; TV, tegmentum vasculosum. Counterstaining of neurofilaments labeled with 3A10 antibody (see A,C,G,H). **Summary table s33–s36 (E8–E10):** See legend to Figure 1 for explanation and font conventions. Scale bar = 100 μm.

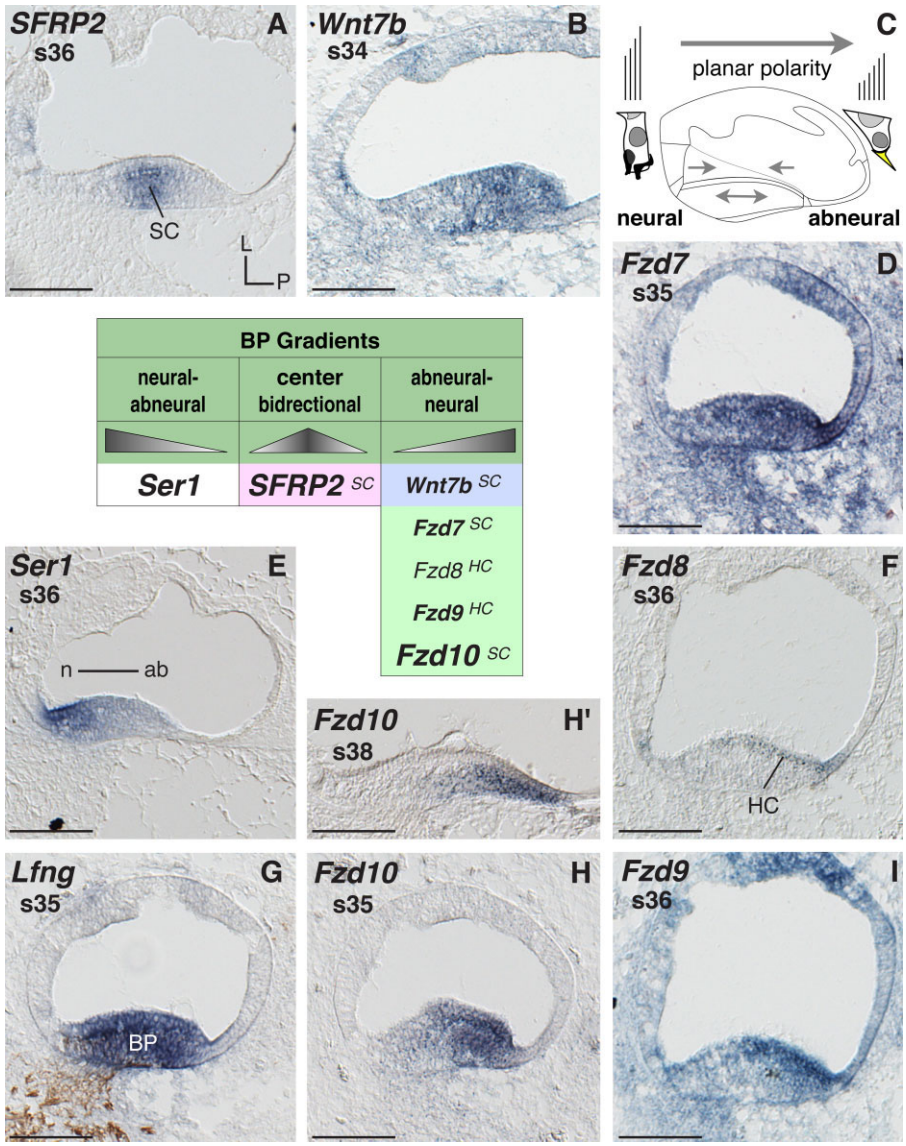

Fig. 4. Basilar papilla mRNA expression. Gene expression in cross sections through the cochlear duct (CD) and basilar papilla (BP). **A,B,D–F,H–I:** BP expresses several genes locally concentrated across the neural-to-abneural axis. **C:** Cartoon cross section of the CD with enlarged neural vs. abneural BP hair cell schematics summarizes the main histological and physiological polarity across the BP (hair cell and bundle shape, innervation, and bundle orientation). Arrows within the CD indicate presumed directional signaling sources based on different gene expression. **G:** Double labeling of the BP (*Lfng* probe) and of neurofilament (antibody 3A10). The table summarizes genes with locally concentrated expressions across the BP. Triangle shapes illustrate the relative signal levels of individual probes. A superscript at the listed gene refers to the main cell type expressing the transcript. Abbreviations: ab, abneural; BP, basilar papilla; HC, hair cells; L, lateral; n neural; P, posterior; s, stage; SC, supporting cells. Scale bar = 100s μm.

BP (Fig. 4A). The other Wnt-related genes with an asymmetric expression pattern are all concentrated on the abneural side of the BP. These are *Wnt7b* (Fig. 4B), *Fzd7* (Fig. 4D), and *Fzd10* (Fig. 4H,H′). Similarly, but more specific to hair cells, this is displayed by *Fzd8* (Fig. 4F) and *Fzd9* (Fig. 4I) at s36 in the BP mid-base. Such local concentration remains, for example, in the case of *Fzd10* at s41 (the latest stage tested; Fig. 4H′ shows s38). A complementary expression pattern, with the highest expression at the neural side of the BP, is shown by the sensory marker, *Ser1*, which is a *Notch* ligand gene (Fig. 3E; this asymmetry contrasts with the other sensory marker *Lfng*, Fig. 4G). Thus, the BP expresses several genes in a radially asymmetric fashion that coincides with the onset of planar cell polarity as well as differentiation of hair cell types (see schematic in Fig. 4C).

In the LM, *Wnt7b* and *Fzd9* (Fig. 3D) overlap with the set of genes described as typical for the auditory organ (excluding *Fzd10* and *SFRP2*; Fig. 3B). In addition, the LM exhibits some faint *Wnt8b* expression (not shown). Parallel to this, all tested Frizzled receptor genes are present (with the exception of *Fzd10*), along with the Wnt-antagonizing genes *Frzb* (Fig. 3I), *Dkk1*, and *SFRP1*. The lagenar transcripts are mostly confined to the differ-

entiating hair cells (Fig. 3D,G–J), with the exception of *Wnt7b*, which populates the entire macula (not shown). *Wnt9a* shows this macular hair cell expression as well (Fig. 3J), although temporally restricted to s34. Of all the expressed genes in LM hair cells, *Frzb* (Fig. 3I) and *Fzd1*, *-2*, and *-7* (Fig. 3G,H) are most striking.

Nonsensory. The nonsensory cochlear duct consists of specialized tissue domains surrounding the sensory organs. These are: the lateral wall of the cochlear duct, which subsequently differentiates into the tegmentum vasculosum and the nonsensory lagenar tissue at the distal end; the homogene and clear cells adjacent to the neural (anterior) side of the BP; and the cochlear limbus tissue on the abneural (posterior) side.

The whole nonsensory cochlear duct domain is broadly occupied by transcripts of the Wnt inhibitor gene, *Frzb* (Fig. 3I). *Wnt6*, which was the main Wnt ligand gene expressed over the length of the nonsensory cochlear duct during earlier stages, is now widely downregulated in this domain beyond s34 (E8) (data not shown). The same seems to be true for *SFRP1*: its expression remains strong only in the proximal cochlear duct (Fig. 3K), the initial region of the forming tegmentum vasculosum and the adjacent differentiating homogene cells. The proximal cochlear duct is where partially overlapping and temporally changing gene expression patterns accompany the specification of these two tissue types (see description of expression boundaries and borders below). From s36 (E10), the tegmentum vasculosum shows regionally strong expression of *Wnt9a*, *Fzd2*, *Fzd9*, *Frzb*, and *Dkk1* (see, e.g., Fig. 5E, *Fzd9*; and 5F, *Wnt9a*).

Signal in the distal nonsensory cochlear duct is considered to belong to the forming lagena. *Wnt4* (Fig. 3M), *Wnt5a*, and *Wnt9a* (Fig. 3E,N) show distinct expression in this area, as does *Wnt11* after s36 (E10; data not shown). As described earlier, *Wnt6* is expressed along the nonsensory cochlear duct overlapping with the nonsensory lagenar domain until s34. *Wnt6* differs from *Wnt4* and the other nonsensory lagenar expressors in that it fails to reach the lateral edge of the macula. The expression of *Frzb*, on the other hand, crosses from the nonsensory cochlear duct over into the sensory lagenar domain (Fig. 3I). The only Frizzled receptor that is transcribed sporadically in the nonsensory lagena is *Fzd4* (not shown).

Along the posterior (abneural) nonsensory cochlear duct, *Fzd8* is expressed (Fig. 3O). Shown later, *Wnt5a*, *Wnt5b*, and *Wnt7a* transcripts are also abundant in this abneural domain (see Fig. 5I, *Wnt7a*; and 5L, *Wnt5b*).

Borders. Expression boundaries and borders in the cochlear duct coincide with: 1) locations of tissue specification; 2) regional compartment separation of the saccule and BP; and 3) the separate fates of cells differentiating in the LM and BP.

Distinctive gene expression patterns in the proximal cochlear duct coincide with the origin of the tegmentum vasculosum and the formation of adjacent homogene cells. Expressions of *SFRP1* (Fig. 3K) and *Wnt4* (Fig. 3L) are both strong in the proximal tegmentum vasculosum at s35, whereas they fade out in the distal direction. However, unlike *SFRP1*, *Wnt4* does not extend into the homogene cell domain, but rather establishes a distinct boundary with it (Fig. 3L). Shortly before the tegmentum vasculosum begins to differentiate, between s32 and s34, the same abrupt boundary adjacent to but excluding homogene cells can also be seen for *Frzb* (Fig. 3I), and three Wnts (*Wnt6*, *-7b*, and *-11*; data not shown). *Wnt11* is notable for its spatiotemporal dynamics as follows: in the proximal tegmentum primordium it forms a blunt demarcation with the homogene cell domain but is clearly excluded from it at s32 (E7.5). Between s34 and early s36, *Wnt11* becomes restricted to a border domain separating the presumptive homogene cells and the tegmentum vasculosum (see under "border: CD/Sac" in Fig. 3 summary table). Curiously then, from s36 onward, *Wnt11* is expressed specifically in homogene cells, which remain positive for *Wnt11* at the latest age tested (s39) (not shown). This means that over time, the expression of *Wnt11* shows spatial changes, being first transcribed in presumptive tegmentum tissue preceding its differentiation, then forming a local border, and finally being expressed specifically by the adjacent tissue type, the homogene cells. The other genes listed above, however, continue to exclude the homogene cell domain. In addition, *Dkk1*, which is expressed in the proximal cochlear duct, becomes downregulated in the homogene cell domain by s37 while continuing its expression in the tegmentum vasculosum (not shown). None of the Frizzled receptors are specifically transcribed in differentiating homogene cells at s33–s36.

The tissues of the proximal cochlear duct represent the remaining connection with the saccule. Thus genes expressed specifically in the homogene cell domain (*Wnt7a*, *-9a*, *-11*, *SFRP1*, and *SFRP2*) contribute to a boundary not only between the BP and the tegmentum vasculosum but also between the BP and the saccule. Likewise, genes expressed locally at the junction of tegmentum vasculosum and homogene cells (*Wnt4* and *Wnt11*) border the nonsensory saccule as well.

At the intersensory border between BP and LM, *Fzd8* transcripts are visible (Fig. 3O). This region also expresses *Wnt4*, *Wnt7a*, *Wnt9a* (Fig. 3N), and *Wnt11* (Fig. 3P). *Wnt9a*, which flanks the LM, extends its expression into the sensory cells of the differentiating LM at s34–s35 (E8–E9; Fig. 3J).

Cochlear cell differentiation at stages 36–41 (E10–E15)

E10–E12 (s36–s38) is a phase when the BP undergoes various cell differentiations. Hair cells and supporting cells become distinguishable by E10 (Cohen and Cotanche, 1992). By E11 (s37), the hair cell stereocilia begin to form a staircase by differential growth in length (Cohen and Fermin, 1978), and a cuticular plate forms at the bundle base. Orientation of hair cell bundles with the kinocillium and the row of longest stereocilia at the abneural side is mainly achieved between E10 and E14 (s36–s40). However, in the midapical BP, a nearly mature bundle orientation is first attained by E18 (s44) and in the distal apex by posthatch day 3 (Cotanche and Corwin, 1991). In particular, the neural apex reorients during the first 30 days after hatching (Cohen and Cotanche, 1992). Thus the main processes of bundle development, rotation, and mature orientation take place from E9 to posthatching day 3 in a spatially specific manner along and across the epithelium (Cotanche and Corwin, 1991). Parallel to the establishment of planar cell polarity, hair cells further differentiate and at E11–E12 (s37–s38), cylindrically shaped tall hair cells, pitcher-shaped short hair cells, and intermediate hair cells, with differential innervation patterns become distinguishable (Cohen and Fermin, 1978). Evi-

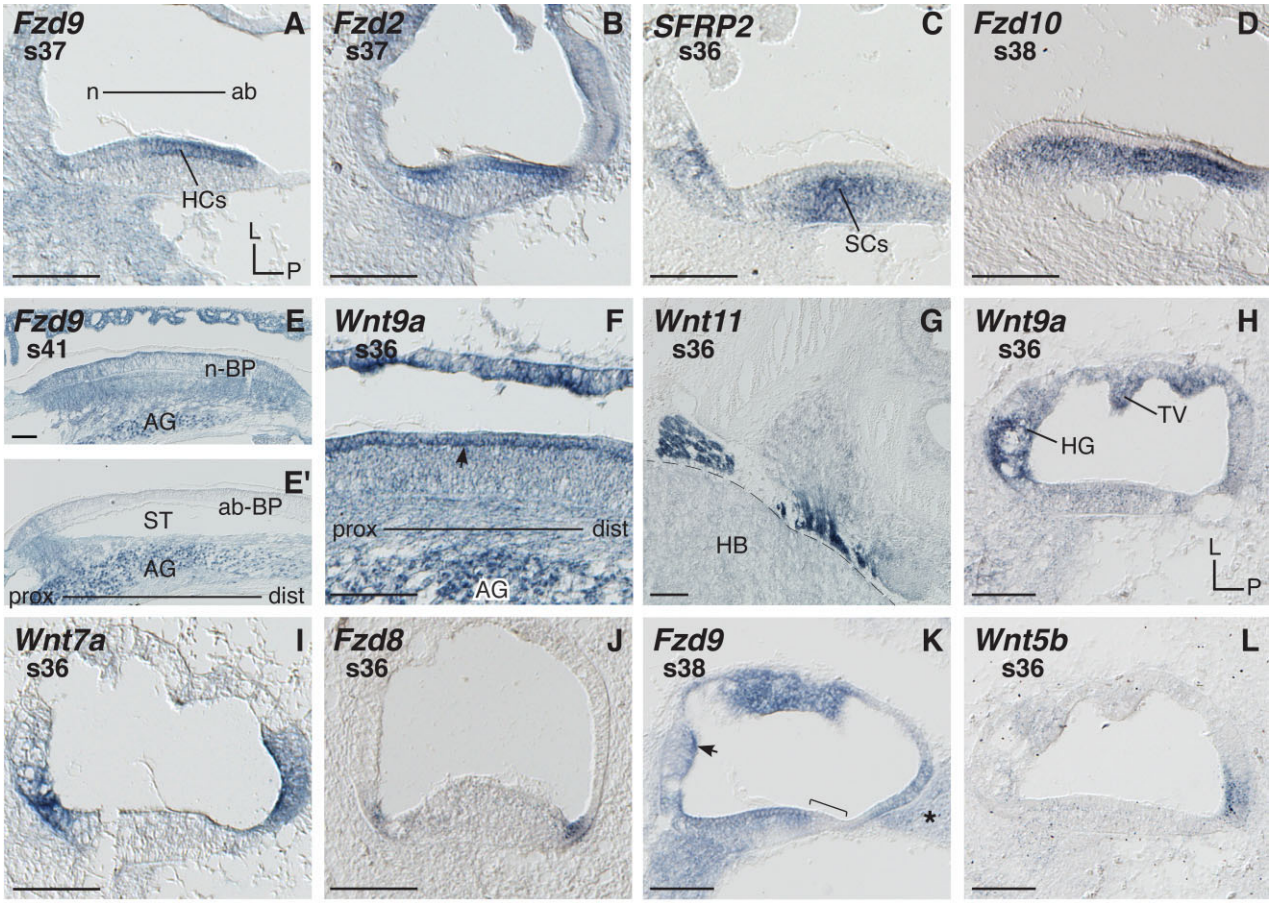

cochlear duct cell types at stages 36-41 (E10-E15)

sensory		nonsensory				
			neural		abneural	
HCs	SCs	TV	HG cells	Clear cells	Border cells	Cuboidal Hyaline cells
Wnt3	***Wnt7b***	*Wnt7b*	***Wnt7a***	***Wnt7a***	*Wnt4*	*Wnt4*
Wnt3a	*Fzd1*	***Wnt9a***	***Wnt9a***	*Wnt9a*	***Wnt5a***	***Wnt5a***
Wnt7b	*Fzd2*	***Fzd2***	***Wnt11***	*Wnt11*	***Wnt5b***	***Wnt5b***
Wnt9a	***Fzd7***	*Fzd7*	*Fzd2*	*Fzd2*	***Wnt7a***	***Wnt7a***
Fzd1	***Fzd10***	***Fzd9***	*Fzd8*	***Fzd8***	*Wnt7b*	*Wnt7b*
Fzd2	***SFRP2***	*Dkk1*	*Fzd9*	*Fzd9*	*Wnt9a*	*Wnt9a*
Fzd4		***Frzb***	*SFRP1*	*SFRP1*	*Fzd1*	*Fzd2*
Fzd7			***SFRP2***	*SFRP2*	*Fzd2*	*Fzd4*
Fzd8					*Fzd4*	*Fzd9*
Fzd9					*Fzd7*	*Dkk1*
Dkk1					***Fzd8***	*SFRP1*
					Fzd9	
					SFRP1	

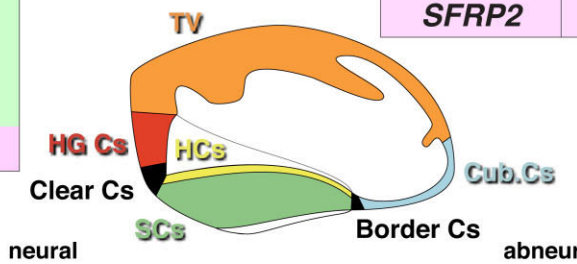

Figure 5

dence of synapses appears with the formation of synaptic bars at E11 (according to Cohen and Fermin, 1978).

The nonsensory cochlear duct is now composed of 1) a neural (superior) domain; 2) the tegmentum vasculosum; and 3) an abneural (inferior) domain forming the limbus. Neurally, homogene cells and clear cells are separating the tegmentum vasculosum from the BP. Abneurally, cochlear tissue differentiates into three cell types. These are the cuboidal cells, hyaline cells and, adjacent to the BP, the border cells. In the differentiating tegmentum vasculosum, dark cells become distinguishable from light cells at s37 (Cotanche and Sulik, 1982), perilymphatic spaces open, and the tectorial membrane is completed (Fermin and Cohen, 1984).

Sensory. The first Wnt-related differential gene expression that discriminates auditory hair cells from supporting cells is shown by *Fzd9* as early as s32 and distinctly at s34 (E8) when transcripts localize to the prospective hair cell layer of the BP (Fig. 3D). This coincides with the identification of hair cells and supporting cells histologically (Cohen and Fermin, 1978; Hirokawa, 1978). The broadly expressed Wnt inhibitor gene *Dkk1* also shows some mRNA accumulation in the hair cell domain at s34 (data not shown). Hair cells preferentially transcribe *Fzd9* (Fig. 5A) and, from s37, *Fzd2* (Fig. 5B). Separation of hair cell and supporting cell layers is established in the BP by s36 (E10), when supporting cells express *SFRP2* (Fig. 5C), *Fzd10* (Fig. 5D), *Wnt7b*, and less distinctly *Fzd7* (data not shown). Before becoming confined to hair cells, *Fzd2* is weakly expressed in supporting cells as well, at least until s36 (not shown). Thus, several genes described before as being characteristic of the BP become restricted later to the supporting cells, with the exception of *Fzd9*, which is restricted to the hair cells. However, in the case of *Wnt7b* and *Fzd7*, this restriction is not perfectly exclusive, especially at s38 (E12) and later, when both genes tend to show some weak expression in the hair cells as well (not shown). By s38/39 hair cells transcribe *Wnt3* and *Wnt3a* (data not shown), genes that were not expressed in the ventral ear before. The expression of *Fzd9* at s36 and s37 tends to be stronger in the abneural BP (Fig. 5A; see also Fig. 4I). However, later (for example, at s38 and s41), when tall hair cells and short hair cells are distinguishable, *Fzd9* remains expressed in the domain of the afferently innervated tall hair cells that is in the neural and middle part of the auditory epithelium (Fig. 5E,K). However, abneural hair cells (short hair cells) do not transcribe *Fzd9* (Fig. 5E′,K, bracket).

At s36 (E10), coinciding with formation of synaptic bars at the base of auditory hair cells, the expression of all genes transcribed in hair cells seems to form a thin line along the hair cell base (Fig. 5F shows this for *Wnt9a*; see arrow). This local mRNA occurrence is detectable for *Wnt9a*, *Dkk1*, and all receptor genes tested (with the exception of *Fzd10*).

Afferent neuronal cell bodies in the auditory ganglion show a distinct expression of *Fzd1*, *Fzd9* (Fig. 5E), and *Dkk1*. Ganglion expression to a varied extent is shown by all tested *Frizzled* receptor genes (with the exception of *Fzd10*), *Frzb*, and *SFRP1*. *Wnt9a*, which is negative for example at s32, is expressed in neuron cell bodies from s34–s35 (E8–E9) onward (Fig. 5F). In addition to the auditory ganglion, the expression of *Wnt9a* is particularly high in other cranial nerve ganglia (not shown). At the border with the hindbrain, Schwann or other glia cells within cranial nerves express three Wnts (*Wnt5a*, *-7b*, and *-11*; Fig. 5G), *Fzd7*, and *Frzb*.

Nonsensory: tegmentum vasculosum. The differentiating tegmentum vasculosum, which was initially positive (s35) for *Wnt4* (Fig. 3L), *SFRP1* (Fig. 3K), and locally restricted *Wnt11*, becomes mostly negative for these genes by s36 (data not shown). At this time, the cells express *Wnt9a* (Fig. 5F,H) and, at least in the proximal region, also *Wnt7b* (data not shown). *Fzd2*, *Fzd9* (Fig. 5E), *Frzb*, *Dkk1*, and *Fzd7* (the latter from s38 onward) are all present in a locally strong and patchy manner that seems characteristic of the tegmentum.

Nonsensory: neural side. Homogene and clear cells in the neural cochlear duct are characterized by *Wnt9a* (Fig. 5H), *Wnt11* (the latter from s36–s37; data not shown) and *SFRP2* (Fig. 5C). *Wnt7a*, which mainly concentrates its neural-edge expression in the clear cells (located between the homogene cells and the BP), shows some extension of its mRNA distribution into the homogene cell domain (Fig. 5I). This overlaps with *Wnt9a* and *Wnt11*, which are mainly expressed throughout the homogene cells but show in some instances their highest expression in the lower half of that domain that corresponds to the clear cells. At s36, a restricted expression of *Fzd8*, and less distinct expression of *Fzd2* and *-9*, demarcate the clear cell domain in some regions of the cochlear duct. For example, *Fzd8* shows a distinct occurrence in the clear cells (and abneural border cells) but only in the basal portion of the papilla (Fig. 5J). Later (s38), the expression of those receptor genes transcribed by homogene and clear cells localizes to the lumenal surface of cells in this tissue (the arrow in Fig. 5K indicates this for *Fzd9*). In addition, the expression of *SFRP1* in the homogene cell domain, described for s35 (see above) remains (latest test s38) but is often also reduced to the subcellular region facing the lumen and the adjacent hair cells.

Fig. 5. Cochlear duct mRNA expressions between s36 and s41 (E10–E15). **A,B,H–L:** Cross sections through the cochlear duct (CD) and basilar papilla (BP). **A,B:** Hair cells expressing *Frizzleds*. **C,D:** Supporting cells transcribing *SFRP2* and *Fzd10*, respectively. **E,F:** Longitudinal sections along the BP. **E,E′:** Neural BP hair cells express *Fzd9* (see E); abneural BP hair cells do not transcribe *Fzd9* (see E′, middle part, where the basilar membrane is situated over the scala tympani). TV cells (see E) as well as afferent cell bodies in the auditory ganglion express *Fzd9*. **F:** Expression of *Wnt9a* 1) in the basolateral region of hair cells (arrow) at s36, 2) TV, and 3) auditory ganglion cell bodies (AG). **G:** Glia/Schwann cells transcribe *Wnt11* at the border to the hindbrain. **H–L:** Cross sections showing gene expression in different cell types of the CD (compare with schema for details). **K:** Arrow indicates lumenal surface of HG cells expressing *Fzd9*; bracket marks abneural BP hair cells negative for *Fzd9* transcription; asterisk marks abneural mesenchyme adjacent to the CD. Abbreviations: ab, abneural; ab-BP, abneural BP; AG, auditory ganglion; Cub, cuboidal; Cs, cells; dist, distal; HB, hindbrain; HCs, hair cells; HG, homogene cells; L, lateral; n, neural; n-BP, neural BP; P, posterior; prox, proximal; s, stage; SCs, supporting cells; ST, scala tympani; TV, tegmentum vasculosum. **Summary table s36–s41 (E10–E15):** See legend to Figure 1 for explanation and font conventions. Scale bar = 100 μm.

Nonsensory: abneural side. Most prominent in abneural tissue domains are *Wnt7a* (Fig. 5I) and *Wnt5a* and *-5b* (Fig. 5L). Their expression labels the complex of cuboidal, hyaline, and border cells. Also prominent is *Fzd8*, yet its expression is restricted to the border cells (Fig. 5J) and may extend into the BP (cf. Fig. 4F), but not hyaline and cuboidal cells. From s38 onward, abneural cells also express *Wnt4*, *-7b*, *-9a*, *Fzd2*, *-4*, *-9* (Fig. 5K shows this for *Fzd9*), *Dkk1*, and *SFRP1*, although in some cases these expressions are comparatively weak. In addition, *Fzd7* and *Fzd1* expression cross from the abneural edge of the BP into the border cell domain (not shown).

Otic mesenchyme (abneural). Located adjacent to hyaline and cuboidal cells, the abneural periotic mesenchyme is the last remaining mesenchyme in the opening perilymphatic space. This tissue shows transcripts of *Fzd9* (Fig. 5K, asterisk) and *Frzb* abundantly and also expresses *Fzd2*, *Fzd7*, and *Dkk1* (data not shown).

DISCUSSION

Wnt-related gene expression in chicken, mouse, and rat inner ears

Our data expand and refine the list of known Frizzled transcripts in the ventral inner ear beyond the otocyst stage. Altogether we find evidence for the expression of seven Frizzled genes during cochlear duct development: *Fzd1*, *-2*, *-4*, *-7*, *-8*, *-9*, and *-10*. *Fzd2* and *Fzd9* are broadly expressed in both prosensory and nonsensory domains (until they become confined to hair cells and later to specific tissue types as, for example, the tegmentum vasculosum). *Fzd1*, *-5*, *-6*, *-7*, and *-10* were previously reported to be transcribed in chicken otic tissue (Lewis and Davies, 2002; Stevens et al., 2003). We show the expression patterns of four additional Frizzleds, including *Fzd2* and *Fzd8*, which were not tested previously, and *Fzd4* and *Fzd9*, which were presumed to be negative. The exclusive transcription of *Fzd10* in the BP reported earlier can now be refined to an earlier time point, as we detected it at s26 (E4–E5), whereas Stevens et al. (2003) did not find *Fzd10* at E4, E5, or E6 but instead described its onset as E7 (s31).

Our analysis reveals the expression of 11 Wnts in the developing ventral inner ear: *Wnt3*, *-3a*, *-4*, *-5a*, *-5b*, *-6*, *-7a*, *-7b*, *-8b* (faint), *-9a*, and *-11*. The vast majority of the Wnt transcripts are present in nonsensory domains, with very few (*Wnt7b* and to a limited extent *Wnt7a*, *Wnt9a*) in the sensory primordia of the BP and LM. We also demonstrate strong expression of the Wnt inhibitors *SFRP2* and *Frzb*, broad expression of *Dkk1*, and variable, mostly weak expression of *SFRP1*. The Wnt inhibitors segregate into subdomains of the ventral ear, possibly to modulate the activity of specific Wnts or Frizzleds at particular times and places.

The chicken expression patterns described here mostly complement previous data from mammals in which Wnts and Fzds were comprehensively studied by transcript profiling. Sajan et al. (2007) found temporally regulated expression of *Wnt7a*, *Wnt4*, and *Wnt5a* in the mouse cochlea by using microarrays. A similar profiling approach for the neonatal mouse cochlea supports expression of 3 to 5 of the 14 Wnt genes present on GeneChips: *Wnt4*, *-5a*, and *-7b* were robust, whereas *Wnt5b* and *-10a* were marginal (Chen and Corey, 2002). Polymerase chain reaction (PCR) amplification of the postnatal rat cochlea shows transcripts of *Wnt2b*, *-4*, *-5a*, *-5b*, and *-7a* in addition to *Fzd1*, *-2*, *-3*, *-4*, *-6*, and *-9* (Daudet et al., 2002). Our data confirm that 8 of these 11 genes are also expressed in the chicken cochlear duct at midgestation; we did not sample *Fzd3* or *Fzd6* and found *Wnt2b* only in the dorsal ear (data to be reported in a separate manuscript). In addition, we report mRNA expression of *Wnt9a* in the chicken inner ear.

Previous in situ hybridization studies of Wnt-related expression in the otocyst indicated that ligands classically associated with β-catenin-dependent canonical Wnt signaling are mostly confined to the dorsal half. Examples include *Wnt2b*, *Wnt3a*, and *Wnt6* (Hollyday et al., 1995; Jasoni et al., 1999; Lillevali et al., 2006). On the other hand, cells that receive canonical Wnt signaling can be traced from their dorsal otocyst origin into the ventral ear in mice (Riccomagno et al., 2005); the purpose of this intriguing migration is still unknown. *Wnt7a* was reported in differentiating pillar cells of the perinatal mouse cochlea (Dabdoub et al., 2003). In the chicken cochlear duct, *Wnt7a* is restricted to the nonsensory flanks of the auditory epithelium, whereas *Wnt7b*'s presence in the abneural half of the BP may be a closer match to the pattern of *Wnt7a* in the mouse cochlea. In both mouse and chicken, *Wnt5b* localizes to nonsensory tissue bordering the auditory epithelium, albeit on both sides in mouse (Daudet et al., 2002) and only abneurally in chicken. Further comparison matches Wnt4 immunoreactivity in the outer spiral sulcus of the mouse (Daudet et al., 2002) to our results of *Wnt4* transcription by abneural border and cuboidal cells at later stages of development (from s38, E12).

Functional data pertaining to the role of Wnt-related genes in cochlear development is mostly confined to the mouse and is still rather limited in scope. *Fzd4* mutant mice show hair cell loss and progressive deafness (Wang et al., 2001; Xu et al., 2004). A pair of Frizzleds, Fzd3 and Fzd6, is involved in hair cell bundle orientation, as indicated by double mutants with disrupted bundle polarity (Wang et al., 2006). In another study of PCP, Qian et al. (2007) demonstrated that Wnt5a antagonizes Frzb in regulating hair cell bundle orientation as well as convergent extension of the cochlea.

Wnt signaling and sensory specification

Stevens et al. (2003) report that the forced expression of canonical Wnt/β-catenin signaling, including Wnt3a misexpression, can induce ectopic sensory patches with LM phenotype in the chicken BP and elsewhere. This observation implies that Wnt/β-catenin signaling is normally kept under tight spatiotemporal regulation, but it also raises the possibility that an endogenous Wnt ligand specifies LM fate. Although *Wnt3a* is not expressed at the appropriate time and place to serve this function, *Wnt4*, *Wnt6*, *Wnt5a*, and *Wnt11* are. All four are present in the distal cochlear duct adjacent to where the LM arises. Wnt4 is known for canonical signaling in other systems, for example, during joint formation (Guo et al., 2004), whereas *Wnt6* signals through the β-catenin-dependent pathway in dermomyotomes (Linker et al., 2005). *Wnt5a* and *Wnt11* are preferentially noncanonical Wnt cues but can also mediate canonical Wnt signaling (Tao et al., 2005; Mikels and Nusse, 2006).

Wnt inhibitors may constrain Wnt-mediated sensory fate specification

If the LM is specified, at least in part, through canonical Wnt signals, how does the nearby BP primordium normally avoid this influence? We note the strong and persistent expression of transcripts for the Wnt inhibitor SFRP2 in the BP primordium but not in the LM primordium. SFRP2 inhibits β-catenin stabilization (Yin et al., 2006) and reduces the activity of Wnt1, Wnt3a, and Wnt4 (Lee et al., 2000; Wawrzak et al., 2007). We wish to speculate that the strong presence of SFRP2 in the BP primordium actively blocks canonical Wnts that may be diffusing from adjacent tissues, or through the cochlear duct lumen, thus preventing the BP domain from initiating an intracellular β-catenin cascade that would otherwise induce the LM vestibular fate. Our hypothesis is supported by the finding that the few Wnts expressed in the BP (*Wnt7b* or *Wnt9a*) that are known to have the ability to signal through β-catenin (Person et al., 2005; Wang et al., 2005) are not transcribed in sensory domains before s34 (E8).

The presumptive homogene cell domain on the neural side of the BP may also need to block canonical Wnt signaling to prevent it from taking on a sensory fate. When challenged with activated β-catenin transgene before s23, these cells are able to convert to a sensory fate (Stevens et al., 2003). The homogene cell domain continuously expresses both *Wnt9a* and *SFRP2*. The SFRP2 inhibitor may be important to commit the homogene cell domain to a nonsensory fate by preventing it from activating a β-catenin response during a critical period at early stages. At s35 (~E9), *SFRP2* is joined by *SFRP1* in the homogene cell region. By s36, homogene and clear cells also express *Wnt11*. Interestingly, Wnt11 is reported to be effective in blocking canonical Wnt signaling (Maye et al., 2004).

Possible autocrine Wnt activity in nonsensory domains

We do not rule out potential roles for Wnt signaling in other parts of the ventral ear, particularly once cell specification and differentiation are under way. In particular, several Wnt genes are ideally placed to play an autocrine role in nonsensory domains, such as *Wnt9a* in the tegmentum vasculosum. Other potential sites of autocrine signaling include border cells, cuboidal cells, hyaline cells, clear cells, homogene cells, and intersensory border regions. On the other hand, nearly all of these emerging cell types also express one or more Wnt inhibitors, which are generally associated with a block of canonical Wnt signaling. Thus, it would appear that either there is tight spatiotemporal regulation of canonical Wnt signaling or there is predominantly noncanonical Wnt signaling in these nonsensory territories.

Wnt signaling sources across the auditory epithelium

A perusal of Wnts previously associated with planar cell polarity (PCP) in other systems reveals several transcripts that unilaterally border the hair cell domains in the BP, including *Wnt5a* on the abneural edge. Wnt5a has been implicated in hair bundle polarity in the mouse (Qian et al., 2007). Other noncanonical spatial asymmetries include an abneural source of *Wnt5b* and a neural source of *Wnt11*. Also notable is the expression of *Wnt7b* in a graded fashion across the BP sensory epithelium from s34 (E8). Wnt7b signals canonically as mentioned before (Wang et al., 2005) but also noncanonically (Rosso et al., 2005; Tu et al., 2007). Furthermore, four Frizzled genes show graded expression across the same axis, from high abneurally to low neurally, with *Fzd10* being the most robust and prolonged, and *Fzd9* as well as *Fzd8* appearing at s36. Fzd10 usually operates in the context of canonical signaling (e.g., Wang et al., 2005). If these Frizzleds are activated by the asymmetrically expressed Wnts, our prediction is that this arrangement would steepen radial Wnt activity gradients originating from the abneural side, while flattening activity gradients from the neural side. A radial gradient of PCP Wnt signaling could contribute to the establishment of bundle polarity (toward the abneural edge). Other spatially graded phenotypes evident in the radial dimension, such as hair cell type (tall hair cells vs. short hair cells) or synaptic terminal size, number, and type (afferents vs. efferents), may utilize either canonical or noncanonical signaling pathways. We note that Wnt expression asymmetries precede both hair bundle polarization (on E9) and the differentiation of tall and short hair cells (on E12).

Superimposed over the radial gradients is the coincident expression of *SFRP2*, with its peak in the center of the BP, which confounds the interpretation. If the purpose of *SFRP2* at this location is to repress canonical signals, such as strong *Wnt9a* arising from the neural side or *Wnt7a* from both sides, then it may simply be permissive for noncanonical signaling across the BP. Alternatively, if any of the bordering Wnts are acting canonically (including possibly Wnt5a), then SFRP2 may sharpen their functional gradients, or it may confine the reach of the bordering Wnt ligands to the cells located on only one half of the BP.

Hair cells on the neural half of the BP will differentiate into hair cells receiving mostly afferent innervation (tall hair cells), whereas hair cells located abneurally will differentiate into hair cells receiving predominantly or only efferent innervation (short hair cells). The presence of neural/abneural asymmetric distributions of both BP innervation and expression of some Wnt-related transcripts highlights a need for determining Fzd protein expression within afferent and efferent growth cones. Wnt3, Wnt4, Wnt5a, Wnt7b, and SFRP1 have all been implicated in axon guidance in other systems, where they can function as either attractants or repellants (Endo and Rubin, 2007).

Whether or how these potential Wnt gradients across the sensory BP may interact with radial expression gradients of two other important ligands, Serrate1 (Fig. 4E) or BMP4 (Cole et al., 2000; Fig. 1D) remains unexplored.

In summary, our data indicate that there are many potential roles for Wnt signaling during development of the ventral ear. These data will provide a baseline for interpreting both gain-of-function and loss-of-function analyses and will facilitate comparative studies for unraveling the role of these genes in cochlear development in other vertebrates, including mammals.

ACKNOWLEDGMENTS

Riboprobes were kindly provided by Susan Chapman, Gary Schoenwolf, Cliff Tabin, Doris Wu, and Julian Lewis. Matías Hidalgo-Sánchez generously shared detailed pro-

tocols. We thank Deborah Biesemeier and Katie Holmes for technical assistance.

LITERATURE CITED

Abu-Elmagd M, Garcia-Morales C, Wheeler GN. 2006. Frizzled7 mediates canonical Wnt signaling in neural crest induction. Dev Biol 298:285–298.

Adam J, Myat A, Le Roux I, Eddison M, Henrique D, Ish-Horowicz D, Lewis J. 1998. Cell fate choices and the expression of Notch, Delta and Serrate homologues in the chick inner ear: parallels with *Drosophila* sense-organ development. Development 125:4645–4654.

Bartolami S, Goodyear R, Richardson G. 1991. Appearance and distribution of the 275 kD hair-cell antigen during development of the avian inner ear. J Comp Neurol 314:777–788.

Cadigan KM, Liu YI. 2006. Wnt signaling: complexity at the surface. J Cell Sci 119:95–402.

Chapman SC, Brown R, Lees L, Schoenwolf GC, Lumsden A. 2004. Expression analysis of chick Wnt and Frizzled genes and selected inhibitors in early chick patterning. Dev Dyn 2293:668–676.

Chen ZY, Corey DP. 2002. An inner ear gene expression database. JARO 3:140–148.

Cohen GM, Cotanche DA. 1992. Development of the sensory receptors and their innervation in the chick cochlea. In: Romand R, editor. Development of auditory and vestibular systems, 2nd ed. Amsterdam: Elsevier. p 101–138.

Cohen GM, Fermin CD. 1978. The development of hair cells in the embryonic chick's basilar papilla. Acta Otolaryngol 86:342–358.

Cole LK, Le Roux I, Nunes F, Laufer E, Lewis J, Wu DK. 2000. Sensory organ generation in the chicken inner ear: contributions of bone morphogenetic protein 4, serrate1, and lunatic fringe. J Comp Neurol 424, 3:509–520.

Cotanche D, Sulik K. 1982. Scanning electron microscopy of the developing chick tegmentum vasculosum. Scan Electron Microsc Pt 3:1283–1294.

Cotanche DA, Corwin JT. 1991. Stereociliary bundles reorient during hair cell development and regeneration in the chick cochlea. Hear Res 52:379–402.

Dabdoub A, Donohue MJ, Brennan A, Wolf V, Montcouquiol M, Sassoon DA, Hseih JC, Rubin JS, Salinas PC, Kelley MW. 2003. Wnt signaling mediates reorientation of outer hair cell stereociliary bundles in the mammalian cochlea. Development 130:2375–2384.

Daudet N, Ripoll C, Molès JP, Rebillard G. 2002. Expression of members of Wnt and Frizzled gene families in the postnatal rat cochlea. Brain Res Mol Brain Res 105:98–107.

Endo Y, Rubin JS. 2007. Wnt signaling and neurite outgrowth: insights and questions. Cancer Sci 98:1311–1317.

Fermin CD, Cohen GM. 1984. Developmental gradients in the embryonic chick's basilar papilla. Acta Otolaryngol 97:39–51.

Fischer FP. 1994. General pattern and morphological specializations of the avian cochlea. Scanning Microsc 8:351–363.

Gleich, O, Fischer, FP, Köppl, C, Manley, GA. 2004. Hearing organ evolution and specialization: archosaurs. In: Manley GA, Popper AN, Fay RR, editors. Evolution of the vertebrate auditory system. New York: Springer-Verlag. p 224–255.

Gordon MD, Nusse R. 2006. Wnt signaling: multiple pathways, multiple receptors, and multiple transcription factors. J Biol Chem 281:22429–22433.

Grier JB, Counter SA, Shearer WM. 1967. Prenatal auditory imprinting in chickens. Science 155:1692–1693.

Guo N, Hawkins C, Nathans J. 2004. Frizzled6 controls hair patterning in mice. Proc Natl Acad Sci U S A 101:9277–9281.

Hamburger V, Hamilton HL. 1951. A series of normal stages in the development of the chick embryo. J Morphol 88:49–91.

Hatch EP, Noyes CA, Wang X, Wright TJ, Mansour SL. 2007. Fgf3 is required for dorsal patterning and morphogenesis of the inner ear epithelium. Development 134:3615–3625.

Hendrickx M, Leyns L. 2008. Non-conventional Frizzled ligands and Wnt receptors. Dev Growth Differ 50:229–243.

Hirokawa N. 1978. The ultrastructure of the basilar papilla of the chick. J Comp Neurol 181:361–374.

Hollyday M, McMahon JA, McMahon AP. 1995. Wnt expression patterns in chick embryo nervous system. Mech Dev 52:9–25.

Jasoni C, Hendrickson A, Roelink H. 1999. Analysis of chicken Wnt-13 expression demonstrates coincidence with cell division in the developing eye and is consistent with a role in induction. Dev Dyn 215:215–224.

Jones T, Jones S. 2000. Spontaneous activity in the statoacoustic ganglion of the chicken embryo. J Neurophysiol 83:1452–1468.

Katayama A, Corwin JT. 1989. Cell production in the chicken cochlea. J Comp Neurol 281:129–135.

Knowlton VY. 1967. Correlation of the development of membranous and bony labyrinths, acoustic ganglia, nerves, and brain centers in the chick embryo. J Morphol 121:179–208.

Lang H, Bever MM, Fekete DM. 2000. Cell proliferation and cell death in the developing chick inner ear: spatial and temporal patterns. J Comp Neurol 417:205–220.

Lee CS, Buttitta LA, May NR, Kispert A, Fan CM. 2000. SHH-N upregulates SFRP2 to mediate its competitive interaction with WNT1 and WNT4 in the somitic mesoderm. Development 127:109–118.

Lewis J, Davies A. 2002. Planar cell polarity in the inner ear: how do hair cells acquire their oriented structure? J Neurobiol 53:190–201.

Li CX, Gong M, Huang YN, Tang ZQ, Chen L. 2006. Morphometry of otoliths in chicken macula lagena. Neurosci Lett 404:83–86.

Lillevali K, Haugas M, Matilainen T, Pussinen C, Karis A, Salminen M. 2006. Gata3 is required for early morphogenesis and Fgf10 expression during otic development. Mech Dev 123:415–429.

Linker C, Lesbros C, Gros J, Burrus LW, Rawls A, Marcelle C. 2005. Beta-catenin-dependent Wnt signalling controls the epithelial organisation of somites through the activation of paraxis. Development 132: 3895–3905.

Manley GA, Haeseler C, Brix J. 1991a. Innervation patterns and spontaneous activity of afferent fibres to the lagenar macula and apical basilar papilla of the chick's cochlea. Hear Res 56:211–226.

Manley GA, Kaiser A, Brix J, Gleich O. 1991b. Activity patterns of primary auditory-nerve fibres in chickens: development of fundamental properties. Hear Res 57:1–15.

Maye P, Zheng J, Li L, Wu D. 2004. Multiple mechanisms for Wnt11-mediated repression of the canonical Wnt signaling pathway. J Biol Chem 279:24659–24665.

Mikels AJ, Nusse R. 2006. Purified *Wnt5a* protein activates or inhibits beta-catenin-TCF signaling depending on receptor context. PLoS Biol 4:e115.

Ohyama T, Mohamed OA, Taketo MM, Dufort D, Groves AK. 2006. Wnt signals mediate a fate decision between otic placode and epidermis. Development 133:865–875.

Perez S, Rebelo S, Anderson D. 1999. Early specification of sensory neuron fate revealed by expression and function of neurogenins in the chick embryo. Development 126:1715–1728.

Person AD, Garriock RJ, Krieg PA, Runyan RB, Klewer SE. 2005. Frzb modulates Wnt-9a-mediated beta-catenin signaling during avian atrioventricular cardiac cushion development. Dev Biol 278:35–48.

Qian D, Jones C, Rzadzinska A, Mark S, Zhang X, Steel KP, Dai X, Chen P. 2007. Wnt5a functions in planar cell polarity regulation in mice. Dev Biol 306:121–133.

Rebillard G, Rubel EW. 1981. Electrophysiological study of the maturation of auditory responses from the inner ear of the chick. Brain Res 229: 15–23.

Riccomagno MM, Takada S, Epstein DJ. 2005. Wnt-dependent regulation of inner ear morphogenesis is balanced by the opposing and supporting roles of Shh. Genes Dev 19:1612–1623.

Rosenhall U. 1970. Some morphological principles of the vestibular maculae in birds. Arch Klin Exp Ohren Nasen Kehlkopfheilkd 197:154–182.

Rosso SB, Sussman D, Wynshaw-Boris A, Salinas PC. 2005. Wnt signaling through Dishevelled, Rac and JNK regulates dendritic development. Nature Neurosci 8:34–42.

Ryals BM, Creech HB, Rubel EW. 1984. Postnatal changes in the size of the avian cochlear duct. Acta Otolaryngol 98:93–97.

Sajan SA, Warchol ME, Lovett M. 2007. Toward a systems biology of mouse inner ear organogenesis: gene expression pathways, patterns and network analysis. Genetics 177:631–653.

Sanchez-Calderon H, Martín-Partido G, Hidalgo-Sánchez M. 2004. Otx2, Gbx2, and Fgf8 expression patterns in the chick developing inner ear and their possible roles in otic specification and early innervation. Gene Expr Patterns 4:659–669.

Sanchez-Calderon H, Martín-Partido G, Hidalgo-Sánchez M. 2005. Pax2 expression patterns in the developing chick inner ear. Gene Expr Patterns 5:763–773.

Saunders JC, Coles RB, Gates GR. 1973. The development of auditory

evoked responses in the cochlea and cochlear nuclei of the chick. Brain Res 63:59–74.

Schambony A, Wedlich D. 2007. Wnt-5A/Ror2 regulate expression of XPAPC through an alternative noncanonical signaling pathway. Dev Cell 12:779–792.

Shiel MJ, Cotanche DA. 1990. SEM analysis of the developing tectorial membrane in the chick cochlea. Hear Res 47:147–158.

Stark MR, Biggs JJ, Schoenwolf GC, Rao MS. 2000. Characterization of avian frizzled genes in cranial placode development. Mech Dev 93:195–200.

Stevens CB, Davies AL, Battista S, Lewis JH, Fekete DM. 2003. Forced activation of Wnt signaling alters morphogenesis and sensory organ identity in the chicken inner ear. Dev Biol 261:149–164.

Storey K, Crossley J, De Robertis E, Norris W, Stern C. 1992. Neural induction and regionalisation in the chick embryo. Development 114: 729–741.

Tao Q, Yokota C, Puck H, Kofron M, Birsoy B, Yan D, Asashima M, Wylie CC, Lin X, Heasman J. 2005. Maternal *Wnt11* activates the canonical wnt signaling pathway required for axis formation in *Xenopus* embryos. Cell 120:857–871.

Tu X, Joeng KS, Nakayama KI, Nakayama K, Rajagopal J, Carroll TJ, McMahon AP, Long F. 2007. Noncanonical Wnt signaling through G protein-linked PKCdelta activation promotes bone formation. Dev Cell 12:113–127.

Vanzulli A, Garcia-Austt E. 1963. Development of cochlear microphonic potentials in the chick embryo. Acta Neurol Latin Am 9:19–23.

Wang Y, Huso D, Cahill H, Ryugo D, Nathans J. 2001. Progressive cerebellar, auditory, and esophageal dysfunction caused by targeted disruption of the frizzled-4 gene. J Neurosci 21:4761–4771.

Wang Y, Guo N, Nathans J. 2006. The role of Frizzled3 and Frizzled6 in neural tube closure and in the planar polarity of inner-ear sensory hair cells. J Neurosci 26:2147–2156.

Wang Z, Shu W, Lu MM, Morrisey EE. 2005. Wnt7b activates canonical signaling in epithelial and vascular smooth muscle cells through interactions with Fzd1, Fzd1, and LRP5. Mol Cell Biol 25:5022–5030.

Wawrzak D, Métioui M, Willems E, Hendrickx M, de Genst E, Leyns L. 2007. Wnt3a binds to several sFRPs in the nanomolar range. Biochem Biophys Res Commun 357:1119–1123.

Whitehead MC, Morest DK. 1985. The development of innervation patterns in the avian cochlea. Neurosci 14:255–276.

Wu DK, Oh SH. 1996. Sensory organ generation in the chick inner ear. J Neurosci 16:6454–6462.

Xu O, Wang YS, Dabdoub A, Smallwood PM, Williams J, Woods C, Kelley MW, Jiang L, Tasman W, Zhang K, Nathans J. 2004. Vascular development in the retina and inner ear: control by Norrin and Frizzled-4, a high-affinity ligand-receptor pair. Cell 116:883–895.

Yin YJ, Katz V, Salah Z, Maoz M, Cohen I, Uziely B, Turm H, Grisaru-Granovsky S, Suzuki H, Bar-Shavit R. 2006. Mammary gland tissue targeted overexpression of human protease-activated receptor 1 reveals a novel link to beta-catenin stabilization. Cancer Res 66:5224–5233.

Zhou W, Lin L, Majumdar A, Li X, Zhang X, Liu W, Etheridge L, Shi Y, Martin J, Van de Ven W, Kaartinen V, Wynshaw-Boris A, McMahon AP, Rosenfeld MG, Evans SM. 2007. Modulation of morphogenesis by noncanonical Wnt signaling requires ATF/CREB family-mediated transcriptional activation of TGFbeta2. Nat Genet 39:1225–1234.